

# Chapter 1

## Introduction

### 1.1 Malaria

Malaria is a disease with severe world-wide implications, with mortality rates approaching 2 million people per year. More than 80% of the world's malaria cases are found in Africa, where at least 800 000 children die from the disease every year (Schapira *et al.*, 1993). A little more than hundred years ago, the use of methylene blue against malaria was described by Guttman and Ehrlich (1891). This was followed by several generations of anti-malarial drugs including: quinine (1820), pamaquine (1924), quinacrine (1930), chloroquine (1934), proguanil (1944), pyrimethamine (1952) and mefloquine (1971). Today the effectiveness of nearly every anti-malarial drug is threatened or impaired by resistant forms of the malaria parasite. Management of the disease has become problematic due to the widespread and steady increase of multi-drug resistant parasitic forms in different parts of the world. This has led to the studies of the mechanisms of drug resistance, and the identification of genetic changes involved in these processes.

The World Health Organisation is currently spending approximately 4% of its budget on anti-malarial activities (Kumar, 1999). Despite these efforts, malaria is now present in 102 countries, and is responsible for 300-500 million clinical cases each year.

Malaria is being virtually ignored by drug companies. Recent facts concerning the American drug industry shed some light on the subject. They invested 10.9 billion dollars in research and development in 1992 (more than twice the amount invested 5 years before). However, the

cost of developing a new drug has more than doubled during the last 10 years. In 1995 it took 231 million dollars, and an average of 12 years to take a chemical from the laboratory to the pharmacy shelf. Using data from the US Army's Anti-malarial Drug Development Program (Brueckner *et al.*, 1998), they show that for every 3000 compounds screened only one reached the final testing stage. Only about half of these final compounds were advanced to preclinical studies. According to the Center for the Study of Drug Development, 5 in 4000 compounds undergoing preliminary testing makes it to the clinical stage, with 1 in 5 of those being approved by the Food and Drug Administration (FDA). It is easy to see that developing new drugs is a very long, high-risk and expensive venture, and that the pharmaceutical industry requires a high return to cover their investment. For comparative purposes, in 1993 the USA was testing 91 AIDS medications, but only one anti-malarial drug was undergoing clinical testing. Malaria is a disease of developing countries, which cannot afford to pay for expensive medicines. This places an enormous responsibility on African scientists to contribute to the search for new anti-malarial drugs in order to reduce the initial costs of the development programme.

The traditional mainstay of anti-malarial treatment, chloroquine, now frequently fails against the *Plasmodium falciparum* malaria parasite, with resistance occurring in South America, Africa and Southeast Asia. Resistant strains of *Plasmodium vivax* have also been reported. Chloroquine resistance has been mapped to a 400 kilobase segment of chromosome 7 in *P. falciparum* (Pennisi, 1999). Chloroquine-resistant parasites rid themselves of the drug 40-50-fold faster than sensitive parasites. Although the exact mechanism of resistance is unknown, it seems to be similar in all strains of the parasite, and is always reversible *in vitro* by verapamil.

South African cultures were analyzed in terms of sensitivity to a range of drugs, including amodiaquine, mefloquine, quinine, chloroquine and sulphadoxine/pyrimethamine (Deacon *et al.*, 1994). These strains were collected from Kwazulu/Natal, and reference strains from South Africa, Malawi and Mozambique were also analyzed.

**Amodiaquine:** All Kwazulu isolates collected from 1984-1986 were sensitive to amodiaquine, but of the 1989-1990 strains, only one was sensitive. Three of the Transvaal isolates from 1987 were amodiaquine sensitive, and two were resistant (Deacon *et al.*, 1994).

**Chloroquine:** Kwazulu-Natal isolates showed 2/14 to be sensitive to chloroquine, comparable to 1987 results when 2/17 and 1988 when 0/14 were sensitive. Chloroquine resistance has risen dramatically since appearing on the African continent in 1978, but remains effective in some regions of Central America, the Caribbean and the Middle East (Deacon *et al.*, 1994).

**Mefloquine:** All strains were sensitive to mefloquine. It should be kept in mind, however, that in Zambia mefloquine resistance was observed ranging between 15% and 48% of isolates. It must also be taken into account that these samples were collected during 1989-1990, and that mefloquine resistance has since been reported. Mefloquine may be used to treat multi-drug resistant malaria, but has been shown to cause neuropsychiatric side effects in some patients (Schlagenhauf, 1999) (Deacon *et al.*, 1994).

**Quinine:** Kwazulu-Natal reference isolates and field strains were shown to have a lower sensitivity to quinine than the four 1990 field isolates. Transvaal and Malawi reference isolates also had reduced sensitivity. Quinine is still used for the treatment of uncomplicated malaria (Raynes, 1999) (Deacon *et al.*, 1994).

**Sulphadoxine/pyrimethamine:** Southern African reference isolates revealed a wide range of susceptibilities. A sharp increase in the amount of drug necessary for IC<sub>50</sub> was shown from 1987 to 1989 in Kwazulu-Natal as well as Transvaal and Malawian isolates. The apparent reduced susceptibility of Kwazulu-Natal isolates could have serious implications for treatment of *P. falciparum* malaria, as this drug combination has been used for treatment in this region since 1988. Combinations of sulfadoxine-pyrimethamine are added to chloroquine treatment when the patient contracted malaria in a region such as South America or Asia (Pearson and Hewlett, 1987)(Deacon *et al.*, 1994).

Polymorphisms in *pfmdr1*, the gene encoding the P-glycoprotein homologue 1 (*Pgh1*) protein of *Plasmodium falciparum*, have been linked to chloroquine resistance; *Pgh1* has also been implicated in resistance to mefloquine and halofantrine. The same mutations influence parasite resistance towards chloroquine in a strain-specific manner and the level of sensitivity to the structurally unrelated compound, artemisinin. Compounds such as doxycycline have a slow but potent action against

the asexual blood stages of *P. falciparum*, as well as the primary intra-hepatic stages (Juckett, 1999). Halofantrine may be used when a poor response to quinine is found, but shows poor and variable absorption and may become toxic (Touze *et al.*, 1997). Artemisinin-based drugs are mostly restricted to the treatment of multi-drug resistant malaria from south-east Asia (White and Olliaro, 1998). The World Health Organisation (WHO) has published guidelines regarding artemisinin use to ensure effective treatment aiming to prevent the fast development of resistance. A summarised diagram of geographical malaria drug resistance is provided in Figure 1.1.

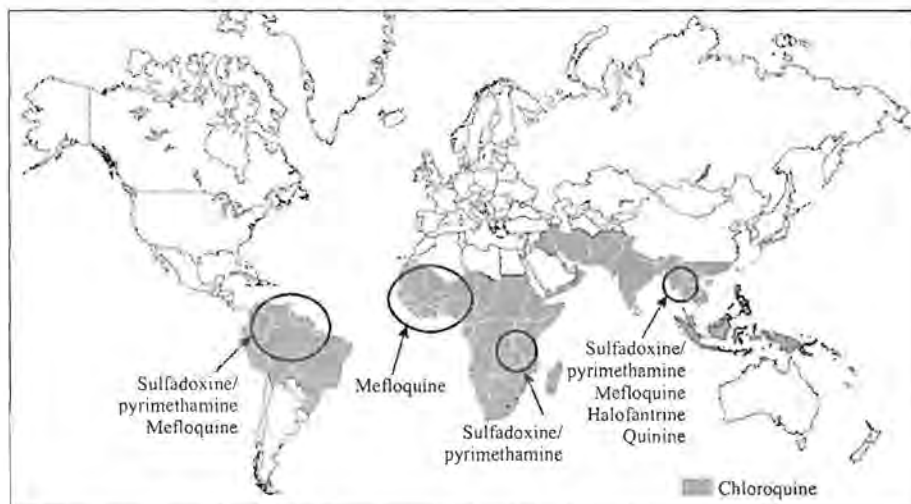


Figure 1.1: Summarised geographical map of recent surveys in malaria drug resistance (Centers for Disease Control and Prevention, Atlanta, 1999).

While various projects are in progress to develop malaria vaccines, realistic estimates put efficient vaccines as far off as 15 years (Holder, 1999). Anti-malarial drugs have contributed heavily towards combatting the disease for the past 100 years, and much potential still exists for developing new drugs against proteins involved in parasite metabolism and invasion. This study will focus on intervention in the major metabolic pathways of *P. falciparum*.

## 1.2 Metabolic pathways

Antiparasitic drugs have been designed to target a series of metabolic pathways (Subbayya *et al.*, 1997). The glycolytic and nucleic acid biosynthesis pathways have been investigated in detail in many parasites, and enzymes from these two pathways will be addressed experimentally in this study. This is preceded by a literature overview of other work done on malaria metabolism and detailed investigations into some potential drug target enzymes.

### 1.2.1 Glycolysis

The malaria parasite lacks a functional tricarboxylic acid cycle and is dependent solely on glycolysis for its ATP requirements (Sherman, 1979)(Roth *et al.*, 1988a)(Roth *et al.*, 1988b). Glucose consumption in *Plasmodium*-infected red blood cells is increased by approximately 50-100 fold over that of uninfected cells (Roth *et al.*, 1988a). The parasite glycolytic enzymes are believed to be associated with membrane components (Dobeli *et al.*, 1991). These enzymes come into contact with the immune system, as antibodies have been found to react to triosephosphate isomerase (TIM) in infected patients (Ritter *et al.*, 1993). Glycolytic enzymes from malaria tend to have a relatively high degree of homology with the human forms. Some of these glycolytic enzymes have been investigated as drug targets. An overview of the glycolytic pathway is given in Figure 1.2.

Hexokinase from *P. falciparum* has 26% identity with the human form, and increased hexokinase activity is found on infection (Olafsson and Certa, 1994). A large C-terminal hydrophobic stretch is present which has been proposed to play a role in membrane association (Olafsson *et al.*, 1992).

Phosphoglucoisomerase (GPI) shows a 4-9 times increase in infected erythrocytes (Srivastava *et al.*, 1992). The expression of GPI parallels parasite maturation and reaches a maximum at the trophozoite / schizont stage. The gene contains a 1773-base pair open reading frame, has no introns, and maps to *P. falciparum* chromosome 14. Of the deduced amino acid sequence, 34% is identical to human glucose phosphate isomerase, with highest similarity in regions of the proposed active sites (Kaslow and Hill, 1990). Gene complementation of an *Escherichia coli*

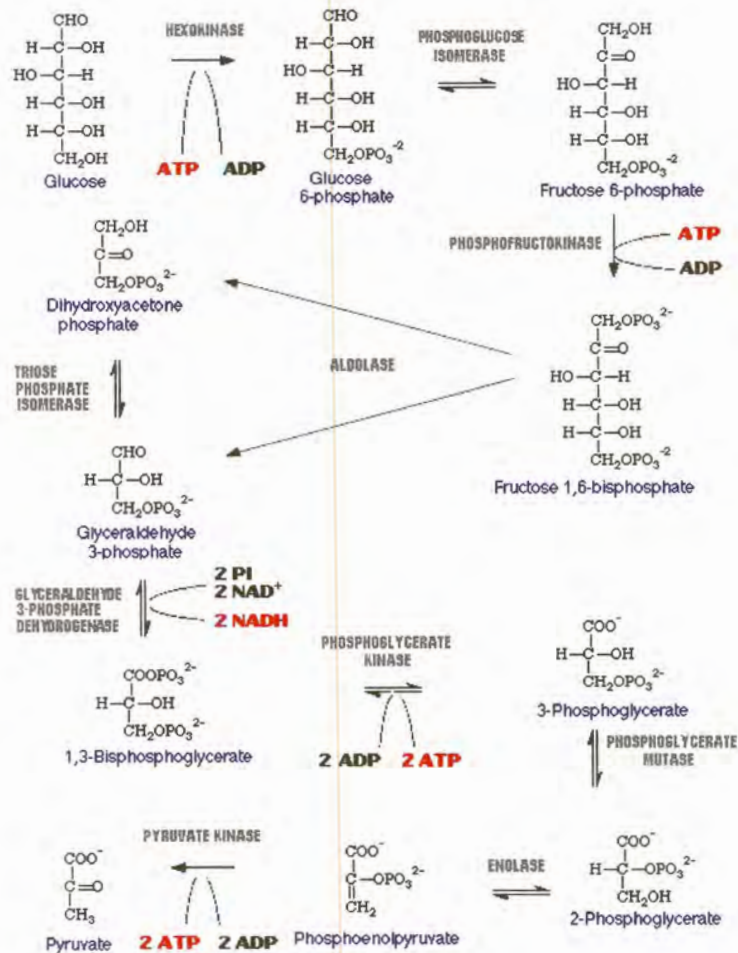


Figure 1.2: The glycolytic pathway

double mutant was used to isolate and express the gene coding for *P. falciparum* glucose phosphate isomerase.

Aldolase is of importance for vaccine development as well as for drug design, since vaccination in monkeys has been shown to offer partial protection (Certa *et al.*, 1988). It shows high sequence homology to human aldolase. Aldolase is known to bind to red blood cell cytoskeletal elements, and the N-terminal end of band 3 is a highly negatively charged inhibitor of aldolase (Dobeli *et al.*, 1990). Inhibitors designed on this basis were unfortunately not selective for *P. falciparum*.

Phosphoglycerate kinase was isolated by Grall *et al.* (1992). The activity of this ATP-generating enzyme in infected red blood cells was found to be 7 times higher than in uninfected cells. Two *P. falciparum* iso-

zymes with neutral isoelectric points were detected.

Lactate dehydrogenase was recently crystallised by Dunn *et al.* (1996). Some features were shown to differ from the human form such as a displacement of the NADH cofactor. A cleft adjacent to the active site was also identified as a possible drug target. The malaria enzyme was selectively inhibited by gossylic nitrile diacetate (GNDA).

Enolase was isolated and characterised by Read *et al.* (1994). All amino acid residues implicated in substrate/cofactor binding and catalysis are conserved in the malarial enolase molecule. The predicted protein sequence displays approximately 60-70% identity to enolase molecules of other eukaryotes. Of particular significance in this well conserved molecule is a characteristic 5-amino acid insertion sequence that is identical in position and virtually identical in primary structure to that which is otherwise found uniquely in plant enolase proteins.

### 1.2.2 Purine salvage pathway

*P. falciparum* like all other parasitic protozoa lacks a *de novo* purine biosynthesis pathway, and obtain purines either by uptake or by a salvage pathway (Sarma *et al.*, 1998).

The major purine source for the parasite is hypoxanthine which is generated from ATP. It is known that the addition of hypoxanthine oxidase to parasite culture medium will lead to the death of parasites (Berman *et al.*, 1991). Since both adenosine and guanosine are formed by the hypoxanthine-guanine phosphoribosyltransferase (HGPRT) pathway via inosine monophosphate, HGPRT would presumably be a good target for antiparasitic drugs. HGPRT was cloned and expressed by Keough *et al.* (1999). Li *et al.* (1999) designed inhibitors corresponding to transition state analogues (the immucillins) which are the most powerful inhibitors yet reported for both human and malarial HGPRTs. Parasite HGPRT has an additional substrate specificity for xanthine, suggesting xanthine analogs as possible inhibitors (Queen *et al.*, 1988). The adenylosuccinate pathway which generates AMP from IMP seems to be unique to parasites, and has been inhibited by the compound hadacidin (Webster *et al.*, 1984). The activity of inosine monophosphate dehydrogenase is inhibited by Bredinin, which affects the formation of GMP from IMP (Scott *et al.*, 1987). Both the aforementioned pathways may be putative targets for selective inhibitors.

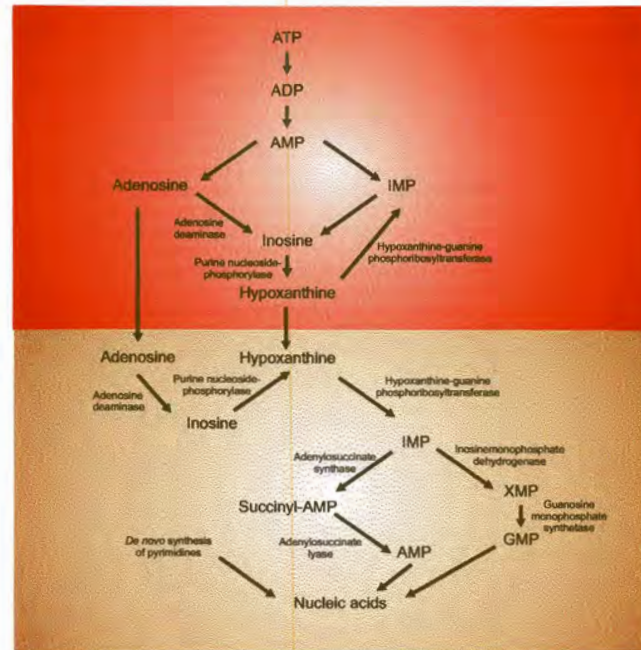


Figure 1.3: The postulated purine salvage pathway in *P. falciparum*. Red indicates the red blood cell pathway and brown that of the parasite.

### 1.2.3 Pyrimidine biosynthesis

The malaria parasite is solely dependent on the *de novo* pathway for pyrimidine synthesis, as they are unable to use a salvage system and human red blood cells contain low pyrimidine levels. Of the enzymes in the *de novo* pathway, carbamoylphosphate synthetase, dihydroorotate dehydrogenase and thymidylate synthase-dihydrofolate reductase have been cloned.

Derivatives of orotate have been shown to inhibit dihydroorotase activity and dihydroorotate dehydrogenase (DHODH), suggesting these enzymes as targets for antiparasitic drugs (Krungkrai *et al.*, 1992). The sequence of DHODH contains an insertion of 42 amino acids compared to the human form. Such insertion events are found in several malaria metabolic enzymes (LeBlanc and Wilson, 1993).

The investigation of malaria metabolic enzymes as new drug targets will hopefully lead to drugs which do not develop resistance within a short time period.

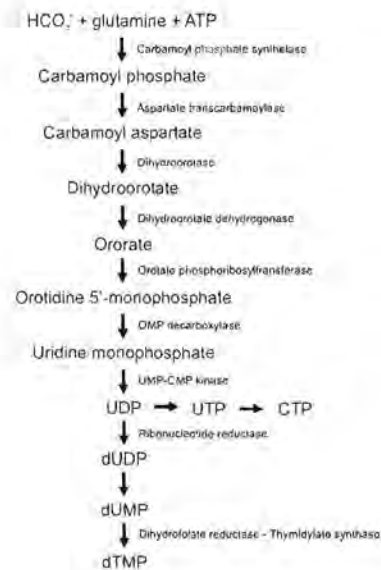


Figure 1.4: *De novo* pyrimidine biosynthesis in *P. falciparum*.

### 1.3 The target enzymes

Dihydrofolate reductase (DHFR) and triosephosphate isomerase (TIM) were chosen as targets for this study. Although malaria DHFR has not been crystallised, the structure has been studied extensively in other species. DHFR has been characterised in detail regarding point mutations leading to drug resistance, and it has been shown that modifications to existing drugs may lead to the return of therapeutical properties. DHFR has been validated as a drug target, and the impact of inhibition has been characterised in detail. TIM from *P. falciparum* was crystallised during the course of this study by Velanker *et al.* (1997). Although TIM has not been validated as a drug target, its structure has been studied extensively in other species, its mechanism is well known and TIM has been subjected to a wide variety of mutational analyses. As a key enzyme in the parasite glycolytic cycle, TIM holds great potential as a putative drug target.

#### 1.3.1 Dihydrofolate reductase

The vitamin folic acid was discovered in 1930, and found to be abundant in leafy foliage, hence the name folic acid (Mathews and Van Holde, 1990). It consists of three moieties: a pteridine ring (6-methylpterin), *p*-aminobenzoic acid (PABA) and glutamic acid (Figure 1.5). Different

numbers of glutamic acid residues may be conjugated to PABA, but animals can only transport the mono-glutamated form. Poly-glutamated folic acid can thus not escape from the cell following conjugation.

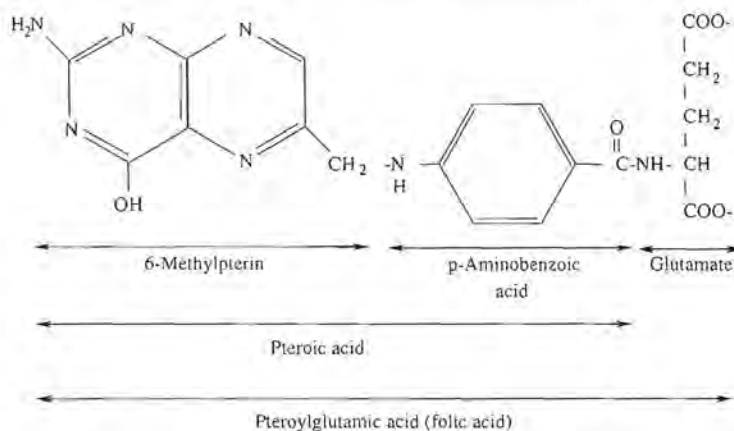


Figure 1.5: Structure of folic acid moieties.

Once inside the cell, folate is converted to active forms by reduction with the enzyme dihydrofolate reductase. The first reduction produces 7,8-dihydrofolate, followed by a second producing 5,6,7,8-tetrahydrofolate (Figure 1.6).

The coenzymatic function of tetrahydrofolate is the mobilisation and utilisation of single-carbon functional groups. These are involved in the amino acid metabolism of serine, glycine, methionine and histidine, as well as purine biosynthesis and methyl group incorporation of thymine.

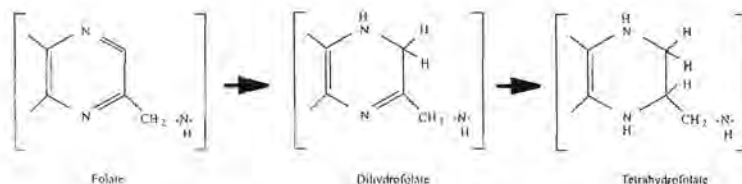


Figure 1.6: Reduction of folic acid.

### Dihydrofolate reductase as a therapeutic target

The enzyme dihydrofolate reductase has been widely studied in a variety of species, including human, chicken and bacterial systems. The malaria DHFR enzyme occurs in the cytosol as a bifunctional complex with thymidylate synthase. The key role of DHFR is in the synthesis

of thymidine, reducing dihydrofolate to tetrahydrofolate (THF) in conjunction with NADPH as cofactor. THF is then further metabolised by thymidylate synthase for the methylation of dUMP to dTMP.

Much attention has been given to the human form of DHFR, because of its use as a chemotherapeutic target in diseases such as cancer. Methotrexate is a potent inhibitor of the enzyme, resulting in inhibition of cellular tetrahydrofolate metabolism and ultimately cell death.

### Human dihydrofolate reductase

The general structure of human dihydrofolate reductase comprises of a larger, as well as a smaller sub-domain, with the active cleft inbetween these two domains. This cleft contains the substrate as well as the NADPH binding sites (Figure 1.7).

The active site comprises of contacts from different parts of the protein's primary structure in a spatial arrangement to yield catalytic activity. Various residues have been implicated in active site contacts.

*Trp24* (red) has been shown to be conserved in all bacterial and vertebrate dihydrofolate reductases. It is part of a loop that connects strand A of the  $\beta$ -sheet and  $\alpha$ -helix B (Beard *et al.*, 1991). Vertebrate DHFRs show a conserved segment of this loop *Pro 23-Trp 24-Pro 25-Pro 26* (red). This loop forms one wall of the active site which is mostly hydrophobic except for *Glu30*. *Trp24* shows hydrophobic and van der Waals interaction with the nicotinamide moiety of NADPH, and its indole nitrogen interacts with the  $C_4$  oxygen of bound folate through a bridge provided by a bound water molecule. The synthetic mutation of this *Trp24* to a *Phe* led to a decrease in substrate affinity and hydride transfer, but an increased  $k_{cat}$  value.

*Phe 31* (yellow) is one of several hydrophobic amino acids lining the active cavity of hDHFR (Chunduru *et al.*, 1994). Previous mutations at this position have shown different and uncorrelated effects on methotrexate binding. The most likely contribution to decreased methotrexate binding is probably due to loss of interaction of the *Phe31* side-chain with methotrexate. The Van der Waals interactions found with the *Phe31* wild type enzyme are not present in mutants containing *Ser*, *Ala* or *Gly*. Similar interactions are found in the wild-type enzyme-folate complex. *Leu*, *Val* and *Gly* mutations may possibly exclude the water molecule. These mutations lead to tight methotrexate binding.



Figure 1.7: Human DHFR (PDB ID: 1DHF) bound to folate. *Trp24* and the conserved loop is indicated in red, *Phe31* in yellow, *Phe34* in green and *Arg70* in cyan. Folate is shown in CPK atom colors.

In each case very little perturbation of the backbone could be shown. However, in each case the presence of an additional molecule of water in the phenyl-occupied cavity could be demonstrated.

One of the components of the catalysis performed by this enzyme is the hydride transfer from  $C_4$  of NADPH to  $C_6$  of  $H_2$ folate, which is critically dependent on the spatial arrangement of the carbon atoms and the relative orientation of the nicotinamide and pteridine rings. This step is speculated to be preceded by an isomerisation concerning the protonation of  $N_5$  of  $H_2$ folate.

*Phe34* (green) is another of the hydrophobic residues lining the active site (Nakano *et al.*, 1994). Its phenyl ring is inclined at about  $45^\circ$  to plane of the pteridine ring of folate, and several atoms of the ring are

in van der Waals contact. A similar structure is found in chicken dihydrofolate reductase. Interaction of the phenyl ring of *Phe34* with methotrexate occurs in a similar fashion as in the case of folate. An investigation was performed where *Phe34* was replaced by smaller residues, and the effect on enzyme activity was studied. Introduction of *Ile*, *Val*, *Thr*, *Ser* or *Ala* at this position led to a marked decrease in affinity for the H<sub>2</sub>folate substrate as well as for methotrexate (Cody and Ciszak, 1991).

*Arg70* (cyan) has been shown to interact with the  $\alpha$ -carboxylate of the terminal L-glutamate of folic acid or methotrexate. X-ray crystallographic data has shown that folate in the active site is directly H-bonded to three conserved hydrophilic residues, of which *Arg70* is one. This residue is invariant in all vertebrate and bacterial DHFR's. Replacement of *Arg 70* by *Lys* led to a significant increase of affinity for methotrexate. Methotrexate is known to bind in the inverse orientation from folate and to be in contact with *Glu 30* via ionic H-bonds. *Ile7* and *Val115* also interact via H-bonds with the 4-amino group of methotrexate (Thompson and Freisheim, 1991).

### ***E. coli* and *L. casei* dihydrofolate reductase**

Li and Benkovic (1992) showed that mutations in the  $\alpha$ -helix of *E. coli* DHFR resulted in an increase in reaction rate, but decreased  $K_m$  and hydride transfer rate. Comparison of the *E. coli* and the *L. casei* structures have shown only 28% amino acid homology, but great similarity in overall structure. The solvent accessible active-site surface of DHFR in *E. coli* is 93% of that of the *L. casei* form. The *E. coli* enzyme is shown in Figure 1.8.

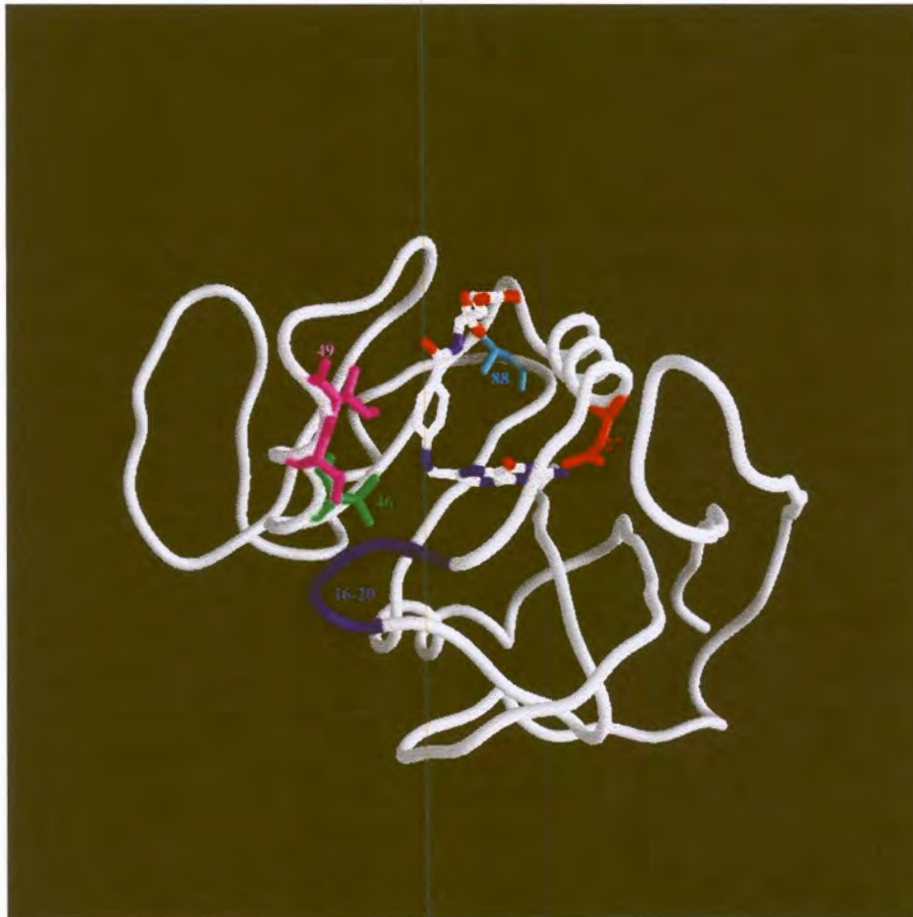


Figure 1.8: *E. coli* DHFR bound to folate (PDB ID: 1DYI). Asp27 is indicated in red, Thr46 in green, Ser49 in purple, Val88 in cyan and the loop formed by residues 16-20 in blue.

The active site of both enzymes is located in a cavity about 15Å deep, lined by mostly hydrophobic amino acids. NADPH binds with the nicotinamide moiety extended through the entrance of the cavity. Methotrex-

ate binds with the pteridine ring nearly perpendicular to the benzoyl ring. The pyrimidine edge of the pteridine ring penetrates into the center of the active site and interacts with *Asp27* (*E. coli*, red) or *Asp26* (*L. cassei*) through hydrogen bonding. *Thr46* (*E. coli*, blue) or *Thr45* (*L. cassei*) is conserved in all known DHFRs and maintains a hydrophobic interaction with the NADPH nicotinamide moiety. Another highly conserved residue is *Ser49* (*E. coli*, purple) or *Ser48* (*L. cassei*) which interacts with N<sub>10</sub>-methyl of methotrexate and with the nicotinamide ribose through hydrogen bonding mediated by a water molecule. The side-chain of *Ile50* (*E. coli*) or *Phe49* (*L. cassei*) is in van der Waals contact with the *p*-aminobenzamide moiety of methotrexate. Near the N-terminus of the enzyme, *Arg44* (*E. coli*) or *Arg43* (*L. cassei*) forms an ion pair with the 5'-phosphate of adenine as well as a hydrogen bond to the ribose via a water molecule. The conserved *Leu54* is located in the loop structure following the helix, and interacts hydrophobically with the *p*-aminobenzamide moiety of methotrexate and is critical in the hydride transfer process.

*Asp27* (red) has been implicated in the hydride transfer process, being the only ionisable group within the active site. It has been proposed to deliver a proton to N<sub>5</sub> of dihydrofolate through a network of water molecules, or act as proton relay with the solvent as source.

Previous work has shown *Asp27* to be critical for catalysis. Dihydrofolate needs to be protonated at N<sub>5</sub> of the dihydropterin ring in order to facilitate hydride transfer from C<sub>4</sub> of the nicotinamide ring of NADPH to C<sub>6</sub> of dihydrofolate. It is still unclear what the immediate source of the proton is, or how it is transferred to N<sub>5</sub> of dihydrofolate, seeing that the carboxylic side-chain of *Asp27* is about 6Å away from the N<sub>5</sub>-C<sub>6</sub> double bond of DHF, and N<sub>5</sub> is buried in a hydrophobic environment composed of *Met20* and *Leu28*. *Asp27* may donate a proton itself, or may catalyze proton donation by a water molecule. The proton may be relayed to N<sub>5</sub> via a fixed water molecule 403, present in every DHFR structure having a ligand in the pteridine binding site. One of the residues that can form a hydrogen bond with water 403 is an invariant *Trp22*. This residue makes hydrophobic interactions with *Met20* and *Leu4* as well as an indirect hydrogen bond with methotrexate through water 403. In the DHFR-NADPH-folate complex, an additional Van der Waals interaction with the nicotinamide is found. *Trp22* (yellow) is also a key residue in the loop connecting βA to αB. This loop serves as a lid closing over bound ligands in the ternary complex. Warren *et al.* (1991)

applied site-directed mutagenesis to the conserved *Trp22* residue. Mutation of *Trp22* to *His* or *Phe* did not however yield the expected results. The water 403 remained unperturbed in the expected position.

Ahrweiler and Frieden (1991) investigated the role of a hinge region with three site-directed mutants at *Val 88*. The turn region reverses the direction of the backbone and separates the molecule into two domain-like structures. In the region following this turn, *Gly95-96* overhangs the methotrexate binding pocket. The carbonyl oxygen of *Ile94* forms a parallel  $\beta$ -bulge with *Gly95*, hydrogen-bonding to  $N_4$  of methotrexate and is proposed to hydrogen bond with  $N_8$  of the dihydrofolate pteridine ring. Site specific mutations disturbed the hydrophobic packing in the *85-91* turn region. A *Val 88* deletion, or mutation to *Ile* or *Ala* led to slight increases in the activity of the enzyme, thus the structure is not yet quite optimal in that region.

Li *et al.* (1992) investigated the role of loop I in DHFR. This mobile loop involves residues 9-24. The central section 16-20 (red) is disordered in the X-ray structure. Binding of folate and  $NADP^+$  causes the disordered segment to form a hairpin turn defined by hydrogen bonding between the backbone carbonyl oxygen of *Met16* and the amino nitrogen of *Ala19*. The newly formed hairpin folds over the nicotinamide moiety of  $NADP^+$  and the pteridine moiety of folate. In the formation of the ternary complex, the loop moves towards the  $\alpha$ -C helix and a hydrogen bond is formed between the side-chain of *Asn18* and the backbone carbonyl oxygen of *His45* in the helix. The bending of the N-terminus of the toward the pteridine binding site causes hydrogen bonding between residues 21 and 24 and a supporting  $\beta$  loop to be moved.

### Avian dihydrofolate reductase

Volz *et al.* (1982) determined the crystal structure of avian dihydrofolate reductase in complex with NADPH and phenyltriazine. The overall backbone folding is very similar to those in other dihydrofolate reductases. The structure of the DHFR-biopterin complex is shown in Figure 1.9.

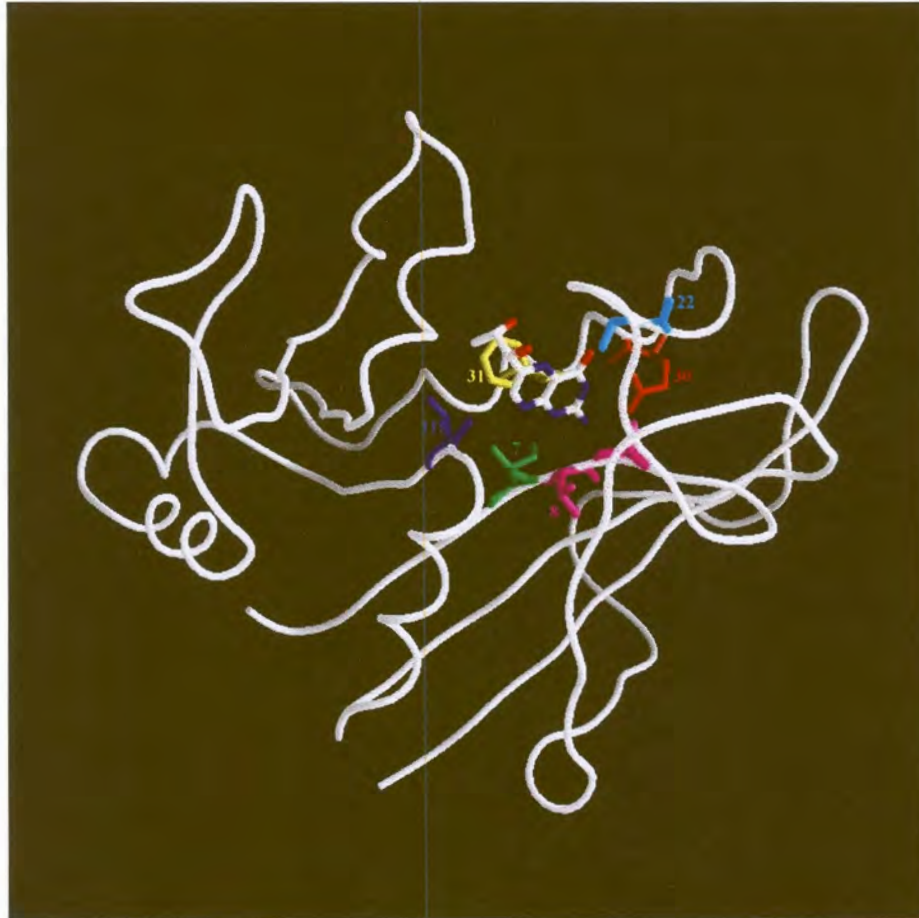


Figure 1.9: Avian DHFR bound to biopterin (PDB ID: 1DR1). *Glu30* is shown in red, *Leu22* in cyan, *Ile7* in green, *Val8* in magenta, *Tyr31* in yellow and *Val115* in blue.

The molecule is folded into an eight-stranded  $\beta$ -sheet consisting of seven parallel strands plus a single anti-parallel strand leading to the carboxy terminus. Four  $\alpha$ -helices are packed against this sheet, while the ones remaining are involved in loops. Avian dihydrofolate reductase contains 189 residues, compared to the 159 in *E. coli* and the 161

in *L. cassei* species. About 70% of the extra residues occur in loops far from the active site.

The carboxyl group of *Glu 30* (red) in the chicken enzyme occupies the same position as *Asp27* in the *E. coli* structure, with the negatively charged carboxylate group in both cases hydrogen-bonded to the ring N<sub>1</sub> and 2-amino group of the respective inhibitors. Lining the binding pocket in hydrophobic contact with the triazine groups are side-chains of *Ile7* (green), the peptide bond between *Val8* and *Ala9*, the side-chains of *Ala9*, *Leu22* (yellow), *Tyr31*, *Phe34*, *Val 115* (blue) and the carboxamide of NADPH. The phenyl ring of *Phe34* is nearly parallel to the triazine ring. The hydroxyl of *Thr136* bonds to a carboxylate oxygen of *Glu30* and to the 2-amino group of the inhibitor, probably via a water molecule. Hydrogen bonds are donated by the 4-amino group of triazine to the carbonyls of *Ile7* and *Val115*. The inhibitor's methoxyphenyl group resides at the mouth of the pteridine binding pocket, analogue to pyrazine and C<sub>9</sub>-C<sub>10</sub> portions of methotrexate. It makes Van der Waals contact with the side-chains of *Leu22*, *Phe34*, *Thr56*, *Ser59*, *Ile60*, *Val115* and the nicotinamide ring of NADPH. *Leu22*, *Ser59* and *Ile60* are structurally equivalent to *Leu29* (*Met20*), *Ser48* (*Ser49*) and *Phe49* (*Ile50*) in the *L. cassei* and *E. coli* structures.

### ***P. falciparum* dihydrofolate reductase**

DHFR in the malaria parasite has been extensively characterised in terms of nucleotide sequences, but little is known of its three-dimensional structure. Sequence characterisation has especially been done to account for parasite resistance to the anti-malarial drugs pyrimethamine and cycloguanil. These drugs were introduced more than 40 years ago, and in combination with sulfa-drugs have been widely used in the treatment of malaria (Peterson *et al.*, 1990). However, the occurrence of resistant strains have been reported. While increased expression of the enzyme may in some cases play a role in drug resistance (Zolg *et al.*, 1989), the major cause is mutations in regions of the enzyme affecting drug binding (Basco *et al.*, 1995).

Proguanil is activated *in vivo* by the mixed function oxidase system of hepatic enzymes to form the active drug cycloguanil. Both cycloguanil and pyrimethamine have been shown to strongly inhibit DHFR ( $K_i$  for cycloguanil =  $0.78 \times 10^{-9}$  M) with a selective anti-malarial action. It

is, however, not known if cycloguanil and pyrimethamine share the same binding site on the enzyme. A wide range of resistance has been demonstrated, with simultaneous mutations (positions 16, 59, 108) leading to resistance against either one, or both drugs at once (Bhasin and Nair, 1996).

De Pécoulas *et al.* (1995) developed a rapid and simple method for the detection of mutations at positions 16 and 108 of *P. falciparum* dihydrofolate reductase. The method consists of the PCR amplification of the DHFR gene, followed by restriction enzyme digestion of codons 16 and 108. Three different enzymes are used to cut the wild-type, the *Thr108* mutant and the *Asp108* mutant. Since every natural antifolate-resistant isolate identified until now carries a mutation in codon 108, determination of this codon can predict the sensitivity of any *P. falciparum* isolate. This technique was employed on local isolates as assayed by Birkholtz *et al.* (1998) to greatly increase knowledge regarding the resistance of *P. falciparum* to pyrimethamine in southern Africa.

Bzik *et al.* (1987) cloned and sequenced the gene for *P. falciparum* dihydrofolate reductase-thymidylate synthase. The amino-terminal DHFR domain was joined to the carboxy terminal TS (thymidylate synthase) domain by a 94-amino acid junction sequence. The TS domain was more conserved than the DHFR domain, and both were more homologous to eukaryotic than prokaryotic forms. The primary DHFR-TS protein contained 608 amino acids, with a calculated mass of 70kDa. The coding sequence resembled other *P. falciparum* sequences in that it had a lower A+T content (75%) than the flanking sequences (94% for 5'-UTR and 87% for 3'-UTR). *P. falciparum* DHFR had little homology to other species in amino acid regions 1-10 and 201-228, while region 11-200 has significant homology except for several amino acid insertions.

Basco *et al.* (1995) studied pyrimethamine and cycloguanil resistant strains, showing a total of 5 amino acid changes. These changes were at *Ala16*, *Asn51*, *Cys59*, *Ser108* and *Ile164*. A single mutation at *Asn108* was associated with moderate pyrimethamine and cycloguanil resistance. Additional mutations at *Asn51Ile* and *Cys59Arg* were required for high resistance to cycloguanil and pyrimethamine. A fourth *Ile164Leu* mutation was observed in a highly resistant Asian strain.

Peterson *et al.* (1990) analyzed cycloguanil resistant *P. falciparum* DNA sequences, finding a Ser to Thr mutation at position 108. This position is usually associated with a Ser to Asp mutation in pyrimethamine resistance. A further Ala to Val mutation was found at position 16. Pe-

terson *et al.* (1988) speculated that the *Asn108* mutation occurs at a site analogous to that of the threonine residue in the C  $\alpha$ -helix of bacterial, avian and human enzymes. *Thr56* in this helix makes contact with the methoxyphenyl group of a triazine inhibitor. The *Asn108* mutation would be expected to affect these kind of contacts and may therefore prevent pyrimethamine binding.

It is of obvious importance that the wide range of contacts described in the previous paragraphs occurring in the human, bacterial and avian forms of dihydrofolate reductase should be taken into account in all studies performed on the *P. falciparum* enzyme. In summary, the most important residues are *Trp24*, *Asp27*, *Phe34*, *Arg70* and *Val115* which interact with the ligand in most of the species studied.

Homology models of malaria DHFR have been prepared by Lemcke *et al.* (1999) as well as Toyoda *et al.* (1997), as discussed in Chapter 3.

### 1.3.2 Triosephosphate isomerase

Triosephosphate isomerase (D-glyceraldehyde 3-phosphate ketol- isomerase; EC 5.3.1.1) is responsible for the interconversion of dihydroxyacetone phosphate and D-glyceraldehyde 3-phosphate. TIM is an enzyme critical for energy production, since no organisms without a TIM gene have been described. A deficiency in TIM leads to chronic hemolytic anemia and neuromuscular disorders (Bardosi *et al.*, 1990).

The cysteine residues of TIM were investigated in the enzymes from *Saccharomyces cerevisiae*, *E. coli*, rabbit, chicken and *Schizosaccharomyces pombe* (Garza-Ramos *et al.*, 1996). Methyl disulfides were produced using phenyl methanethiosulfonate. No effect was found on *S. cerevisiae* and *E. coli*, but the chicken and *S. pombe* were inhibited. It was found that the enzymes having a Cys in position 217 were sensitive to MePhSO<sub>2</sub>-Ph treatment.

#### Human triosephosphate isomerase

An overview of the structure of human TIM complexed to the active-state analogue, phosphoglycolic acid (PGA) is shown in Figure 1.10, and the TIM active site region is depicted in Figure 1.11.

The mechanism of the TIM reaction has been studied over the years and may be summarised as follows (Aqvist and Fothergill, 1996): After binding of DHAP one of the C-1 protons is removed by the *Glu165* (red) catalytic base, yielding the corresponding enediolate. It is then protonated at O-2 by the imidazole ring of *His95* (green), yielding a double protonated enediol and a imidazolate ion. This is followed by the recapture of a proton by *His95* from the O-1 oxygen creating an enediolate lacking the proton at O-1. Protonation of the enediolate occurs at C-2 by the carboxyl group of *Glu165*, thus restoring the general base to release the D-GAP product. The proximity of *Lys12* (blue, forming an ion bond with *Glu165*) to the substrate together with hydrogen bonds from *His95* and *Asn10* (purple) are important in stabilising the enediolate species. The  $\alpha$ -helix directed at *His95* also contributes to the stability of the imidazolate ion (Lodi and Knowles, 1993). Simulations have indicated that a water molecule situated between *Glu165* and *His95* plays an important role during catalysis, providing stabilisation by hydrogen-binding to *Glu165*, the substrate and negatively charged *His95*. Investigation of a *Ser96Phe* mutant showed that cat-

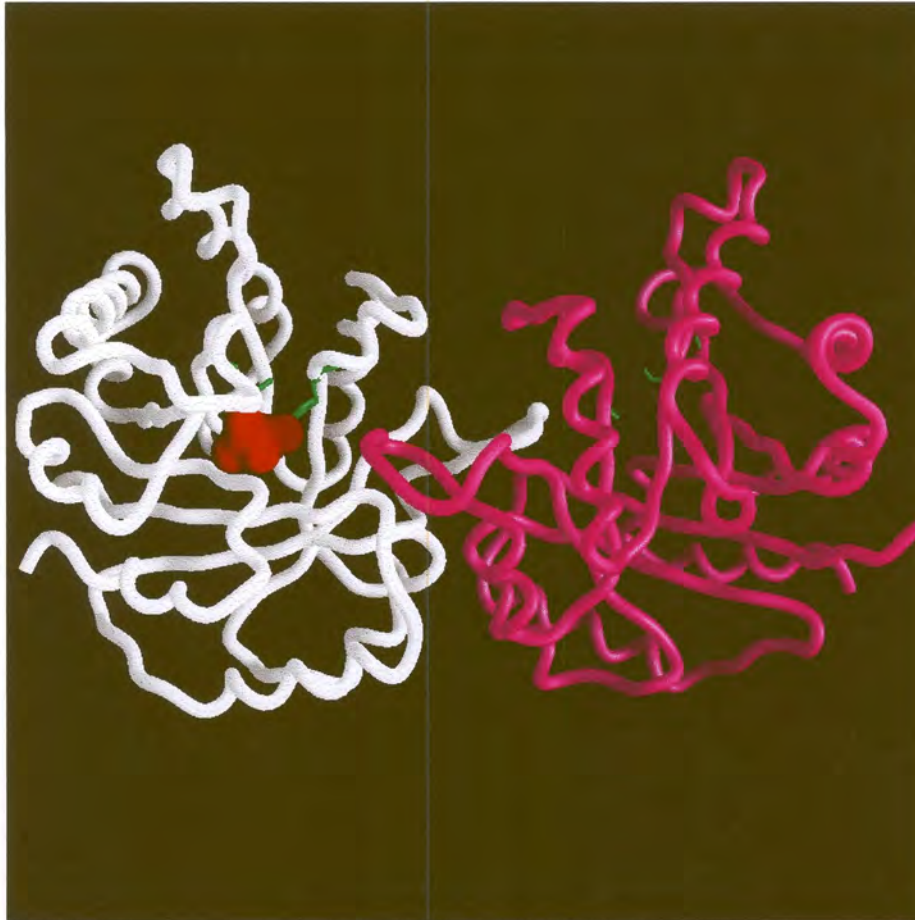


Figure 1.10: Dimeric human TIM with the active sites of both subunits indicated in green (PDB ID: 1HTI). PGA is shown in red in the active site of one subunit.

alytic activity was dramatically decreased, and that this was probably due to the displacement of a water molecule. *Thr75* (yellow) from the second subunit donates a hydrogen bond to the carboxylate group of *Glu97* (cyan) when *His95* is neutral. This is probably one of the reasons for the low activity of monomeric TIM (Borchert *et al.*, 1994).



Figure 1.11: An overview of the human TIM active site region (PDB ID: 1HTI). PGA is shown in CPK colours. *Glu165* is shown in red, *His95* in green, *Lys12* in blue, *Asn10* in purple and *Glu97* in cyan. *Thr75* and its chain from the second subunit are shown in yellow.

### Yeast triosephosphate isomerase

TIM from yeast was first crystallised by Lolis *et al.* (1990). It was shown to be active only in dimeric form (Waley, 1973). The active site structure is shown in Figure 1.12.



Figure 1.12: The active site region of yeast TIM (PDB ID: 2YPI). *His95* is indicated in red, *Glu165* in green, *Lys12* in cyan, *Glu97* in blue and residues 71-77 in magenta. PGA is indicated in CPK colours.

The imidazole  $N_{\epsilon}$  of *His95* was within hydrogen bond distance ( $3\text{\AA}$ ) of a solvent oxygen and a carboxylate oxygen of *Glu165* (green,  $3.3\text{\AA}$ ). Since the carboxylate was unprotonated and both water and the glutamate side-chain may act as hydrogen bond acceptors, it was concluded that the  $N_{\epsilon 2}$  of *His95* (red) was the hydrogen bond donor and was thus protonated. The  $N_{\delta 1}$  atom is within hydrogen bond distance of the backbone amide nitrogen of *Glu97* (blue). Stereochemical restraints

dictate that the amide nitrogen must be the proton donor and the N $\delta$ 1 the acceptor. The N $\delta$ 1 is thus unprotonated and the imidazole in an uncharged state. The major contacts of the subunit interface were at residues 71-77 (magenta), extending from one subunit into a pocket near the active site of the other subunit. This area is in general more hydrophobic than the rest of the monomer surface. At the interface, 15 water molecules were found of which 10 mediated interaction between the subunits. Little sequence conservation between species occurs at the interface, and the authors speculated about the possibility of designing selective inhibitors preventing TIM dimerisation. A study by Lodi *et al.* (1994) emphasised the importance of a positively charged active site. This was supported by mutation of *Lys12* to *Met* giving rise to a loss in enzyme activity. Substitution with amino acids carrying a positive charge or having the potential to be positively charged, resulted in lower enzymatic activity. The TIM-2-phosphoglycolic acid complex was crystallised (Lolis and Petsko, 1990), and showed that PGA formed hydrogen bonds to the side-chains of *His95* and *Glu165*, confirming that *Glu165* is protonated upon PGA binding. Conformation changes induced by binding were the movement of the *Glu165* side-chain by 2Å and the movement of a 10-residue flexible loop 7Å closer to the active site. This so called "hinged lid motion" closes over the active site upon binding, providing a "hinged lid" structure (Joseph *et al.*, 1990). Crystallisation of the TIM-phosphoglycolohydroxamate complex suggested the mechanism whereby the carboxylate of *Glu165* removes a proton from C1 of DHAP while *His95* donates a proton to the DHAP oxygen to form an enediolate intermediate (Davenport *et al.*, 1991). When *Glu165* was changed to *Asp*, the distance to the substrate increased by 1Å, but the major impact was to decrease catalytic activity due to differences in orientation of the catalytic groups (Joseph-McCarthy *et al.*, 1994).

### **Avian triosephosphate isomerase**

The crystal structure of chicken TIM was determined as early as 1975 by Banner *et al.* (1975). They showed two roughly spherical subunits with a diameter of approximately 35Å each. An inner barrel fold with 8 strands of parallel pleated  $\beta$ -sheets was visible. The TIM-PGH complex was crystallised by Zhang *et al.* (1994), and compared to the uncomplexed structure. The model of TIM-PGH was similar to that obtained for both unliganded avian TIM and TIM from yeast. Upon binding to PGH, the carboxylate group of the catalytic base *Glu165* was shown to

move 2-3Å toward PGH. In the free enzyme, the carboxylate is oriented deeper in the active site pocket, and the carboxylate oxygens form two hydrogen bonds with the backbone amide nitrogen and the side-chain hydroxyl group of *Ser96*. After PGH binding, these hydrogen bonds are broken and the *Glu165* (green) side-chain moves into proximity of PGH (Figure 1.13).

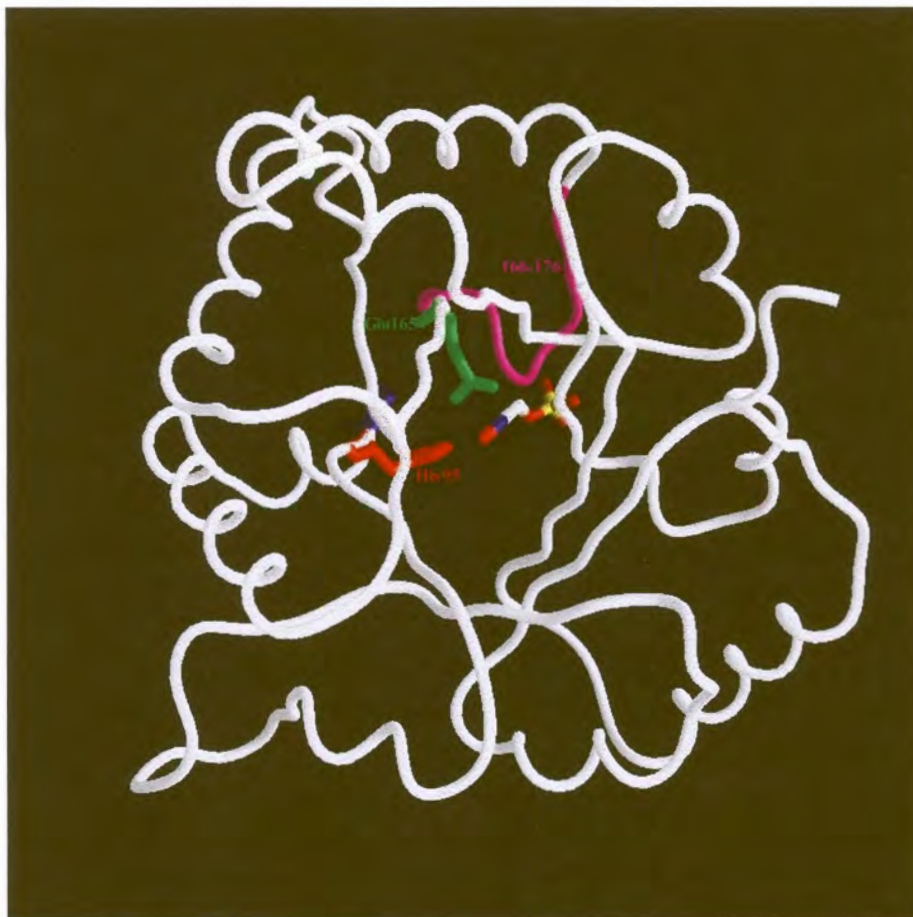


Figure 1.13: The active site of avian TIM (PDB ID: 1TPH). *His95* is indicated in red, *Glu165* in green and residues 166-176 in magenta. PGH is shown in CPK colours.

The loop of residues 166-176 (magenta) in the unbound state is exposed to solvent, leaving the active site accessible to the substrate. In the complex, the loop closes over the active site acting like a rigid lid.

### ***Trypanosoma* triosephosphate isomerase**

The TIM enzyme from *Trypanosoma brucei* was crystallised by Wierenga et al. (1984). Residues involved in catalysis are conserved between TIM of most species, decreasing the chances of developing selective inhibitors (Kuntz et al., 1992). Three loops are of importance in the formation of dimeric TIM, as indicated in Figure 1.14.



Figure 1.14: Structure of *Trypanosoma* TIM (PDB ID: 4TIM). *Lys13* is indicated in cyan, and *His95* in yellow. Loop 1 is colored blue, loop 2 green, loop 3 red and loop 4 magenta.

Loop 3 (red) is relatively long, with the tip around *Thr75* fitting into a cavity near the classical  $\beta$  turn. A series of cyclic peptides were designed to mimic the loop-2  $\beta$ -turn (green), but no inhibition of enzyme activity could be shown. A second series of more hydrophobic cyclic peptides were able to inhibit the TIM from *Trypanosoma brucei*, but not

from other species such as rabbit, yeast and *E. coli*. The inhibition was non-competitive and reversible, and it was shown that more than one peptide could bind per active site. The anti-trypanosomal drug Suramin appeared to compete with the enzyme's substrates ( $K_i = 0.1\text{mM}$ ), indicating an influence at the active site. Inhibition was not present at an ionic strength above 0.01M (Lambeir *et al.*, 1987).

In dimeric TIM, loops 1 (blue) and 4 (magenta) are very rigid due to interaction with the other subunit. In monomeric TIM *Lys13* (cyan) and *His95* have been shown to be more flexible. By point mutation, these two residues were shown to be essential for optimal catalysis (Schliebs *et al.*, 1996). The *Lys13Ala* mutant was completely inactive although still being able to bind substrate analogues. The *His95Ala* mutation was 50 times less active than the wild-type enzyme.

In summary, *Lys12*, *His95*, *Glu165* and *Thr75* play a major role in the catalytic process, and should be taken into account in any contacts identified during ligand searching and design.

### ***Plasmodium falciparum* triosephosphate isomerase**

Triosephosphate isomerase from *Plasmodium falciparum* was first cloned and sequenced by Ranie *et al.* (1993). A cDNA library was used as initial source. TIM cDNA contained a 5'-untranslated region of 172bp, followed by an open reading frame of 744bp which showed an AT-content of 71%. The features surrounding the start codon correlated well with that found for other *P. falciparum* genes, with an adenine preceding the ATG followed by a purine (Robson and Jennings, 1991). A 42-45% sequence identity was seen with higher and lower eukaryotes, and 40% with bacteria with active site residues being conserved in comparison to yeast, chicken and *Trypanosoma*. Significant variance in comparison to the human TIM active site region was *Ala73Ser*, *Phe75Tyr*, *Ser96Phe*, *His100Lys*, *Val101Tyr*, *Lys130Ser*, *Val167Leu* and *Gly233Asn*. Upon investigation of the *P. falciparum* genomic DNA, an intron of 309 bp was found in the codon for residue 38. Like all introns it begins with GT and ends with AG. The intron was shown to be 86% AT-rich. In comparison, TIM from maize contains 8 introns (Marchionni and Gilbert, 1986), but the location of the *P. falciparum* intron is conserved in chicken (Straus and Gilbert, 1985), human (Brown *et al.*, 1985), rhesus monkey (Old and Mohrenweiser, 1988), chimpanzee (Craig *et al.*, 1991) and maize. The enzyme from

*P. falciparum* was overexpressed using the pTrc99A plasmid in *E. coli* AA200 which is TIM deficient. Large amounts of a 28kDa protein were visible, and the specific activity in crude lysates was four times higher than in the control *E. coli* which was TIM deficient (Ranie *et al.*, 1993).

## 1.4 The approach

The identification of new inhibitors is enhanced by structural modelling of the target proteins. Detailed characterisation of the enzyme's active sites may be used in rational approaches to drug screening of chemical software libraries and *de novo* design of new inhibitory compounds. Once ligands have been selected, *in vitro* and *in vivo* screening is needed to evaluate the potential of these compounds as possible lead drugs. In summary, the following approaches were followed in this study as discussed in the successive chapters:

- Cloning, expression, characterisation and purification of the two putative malaria drug target enzymes, dihydrofolate reductase and triosephosphate isomerase.
- Homology modelling of dihydrofolate reductase and triosephosphate isomerase.
- Ligand docking and *in vitro* ligand screening of selected compounds binding to malaria triosephosphate isomerase, and *in vivo* screening of malaria cultures.

## Chapter 2

# Expression of putative malaria drug target proteins

### 2.1 Introduction

A large amount of a pure functional protein is required for a study involving inhibitors of an enzyme. Such quantities can usually only be produced by recombinant overexpression of the enzyme. The recombinant expression of *P. falciparum* proteins has met with problems in many different expression systems. The AT-nucleotide ratio of the malaria parasite varies from approximately 86% in non-coding regions to 69% in coding regions (Weber, 1987). This has clear implications on the tRNAs necessary for translation of these proteins (You *et al.*, 1999). The tRNA repertoire of an organism is optimised for the codons most often used for an amino acid, and the introduction of a gene employing different codons may lead to the exhaustion of certain tRNAs. Some promoters seem also to discriminate against the expression of malaria genes. This may be rectified in different ways. A popular approach is the preparation of whole synthetic genes (Sirawaraporn *et al.*, 1993)(Sano *et al.*, 1994). Oligonucleotides in the range of 50-150 bases are assembled either by restriction digestion followed by ligation, or alternatively by PCR-based methods. These synthetic genes were designed to utilise codon preferences of the expression host organism,

and also to take into account any start codon preferences of the promoter used. A recent alternative is to co-transfect the organism with a vector encoding the necessary tRNAs for supplementation purposes (You *et al.*, 1999).

Once translation of the malaria protein has been achieved, the next challenges are those of correct folding and solubility. Especially in bacterial systems, foreign proteins do not always fold correctly and these misfolded proteins tend to form intra-cellular inclusion bodies. The lack of chaperones may play a role in the incorrect folding of some proteins. The presence or absence of chaperones in malaria have not been conclusively proven but chaperone-like proteins have been found (Hassoun *et al.*, 1998)(Foley *et al.*, 1994). The overexpression of large quantities of a recombinant protein may also overload the cellular mechanisms and cause precipitation of a fraction of the protein which can not be accommodated in the cytosol. This may be optimised in several ways. One is to use a tightly controlled promoter, which does not allow any leaky expression in the uninduced stage (Studier *et al.*, 1990). Expression is then induced in a slow manner, so that large amounts of proteins do not suddenly accumulate in the cytosol. The growth of bacteria at lower temperatures has been shown to have a large effect on the solubility of recombinant proteins, probably due to the speed of growth, protein synthesis and also the protein conformation at lower temperatures (Song *et al.*, 1999). Some proteins which were insoluble at 37°C were successfully expressed at 25°C or 30°C.

Various systems have been used for the expression of malaria proteins such as *E. coli* (Sirawaraporn *et al.*, 1993), yeast (Bathurst, 1994), COS cells (Elliott *et al.*, 1990), *Dictyostelium discoideum* (Fasel *et al.*, 1992) and recombinant baculovirus-infected cultures (Matsuoka *et al.*, 1996). Some yeasts have very high AT-ratios similar to *P. falciparum* which may simplify the expression of malaria proteins. Bacterial systems remain the most economic and simple way for expression, as long as the proteins can be expressed in a suitable form for further use. For the purposes of vaccine development the protein may not necessarily need to retain full activity, but for use in drug screenings and mutational studies, the characteristics should be as close as possible to the native parasite protein. Some malaria metabolic enzymes that have been successfully expressed in recombinant systems are listed in Table 2.1.

From this list it can be clearly seen that *E. coli* is by far the most popular expression system for *P. falciparum* genes. Therefore, any global op-

Table 2.1: Some malaria enzymes which have been successfully expressed in recombinant systems.

Enzyme	Organism	Reference
Dihydrofolate reductase (DHFR)	<i>E. coli</i>	Sirawaraporn and Yuthavong (1986)
Triosephosphate isomerase	<i>E. coli</i>	Ranie <i>et al.</i> (1993)
Falcipain	Bacullovirus	Salas <i>et al.</i> (1995)
Adenine phosphoribosyltransferase	Mouse L cells	Pollack <i>et al.</i> (1985)
Antigens	Yeast	Bathurst (1994)
Circumsporozoite protein	<i>Dictyostelium discoideum</i>	Fasel <i>et al.</i> (1992)
Ookinete surface antigen	Bacullovirus	Matsuoka <i>et al.</i> (1996)
Lactate dehydrogenase	<i>E. coli</i>	Bzik <i>et al.</i> (1993)
Glutamate dehydrogenase	<i>E. coli</i>	Penny <i>et al.</i> (1998)
ADP-ribosylation factor	<i>E. coli</i>	Steketee <i>et al.</i> (1996)
Plasmepsin I	<i>E. coli</i>	Moon <i>et al.</i> (1997)
S-adenosylhomocysteine hydrolase	<i>E. coli</i>	Creedon <i>et al.</i> (1994)
Dihydrofolate reductase - thymidylate synthase	<i>E. coli</i>	Prapunwattana <i>et al.</i> (1996)
Glucose phosphate isomerase	<i>E. coli</i>	Kaslow and Hill (1990)
Hypoxanthine-guanine phosphoribosyltransferase	<i>E. coli</i>	Vasanthakumar <i>et al.</i> (1990)
Aldolase	<i>E. coli</i>	Dobeli <i>et al.</i> (1990)

timisations that can be made for *E. coli* expression would be extremely valuable.

The purification of the recombinant protein may present a problem, especially if an expression host possessing a protein very similar to the recombinant one is used. The ideal solution is the addition of some sort of a peptide tag selective for the recombinant product as a fusion protein, such as a poly-histidine tag, a S-tag (Richards *et al.*, 1972) or an antibody epitope tag (Enomoto *et al.*, 1998). These tags do not usually interfere with the correct folding of the protein and can often be removed after purification by protease cleavage.

If the recombinant protein can not be successfully expressed in a soluble form, methods exist for purifying the protein from inclusion bodies in a denatured form (Mukhopadhyay, 1997)(Lin and Cheng, 1991). The denatured protein may then be renatured by dialysis or other slow solvent exchange methods. In the case of malaria DHFR, the protein was denatured with guanidinium chloride, and subsequently renatured by dialysis to remove the strong denaturant. For example with histidine-tagged proteins, methods are available for renaturation during the column purification procedure (Lin and Cheng, 1991).

This chapter addresses the following goals:

- The optimisation of *E. coli* expression systems for malaria metabolic enzymes.
- The expression of *P. falciparum* DHFR in an active soluble form.
- The purification and characterisation of *P. falciparum* DHFR.
- The cloning of *P. falciparum* TIM cDNA.
- The expression of *P. falciparum* TIM.
- The purification and characterisation of *P. falciparum* TIM.

## 2.2 Materials and Methods

### 2.2.1 Expression of dihydrofolate reductase

#### 2.2.1.1 The pET17 system

pET17 plasmid containing a synthetic gene for *P. falciparum* DHFR was a kind gift from the group in Thailand (Sirawaraporn *et al.*, 1993). pET17-DHFR was propagated in *E. coli* strain BL21(DE3) (Novagen, Madison) using Luria-Bertani (LB)-broth containing carbenicillin (50 µg/ml). Cultures were grown to an OD<sub>600nm</sub> of 0.8, and expression was induced by the addition of IPTG to a final concentration of 0.4 mM. Cultures were grown for 4 hours post-induction, and bacteria harvested by centrifugation. The pellet from 1 ml of culture was washed in 50 mM Tris pH 7.4 (500 µl), and resuspended in H<sub>2</sub>O (25 µl). An equal volume of 2x SDS loading buffer (100 mM Tris pH 6.8, 200 mM DTT, 4% SDS, 0.2 bromophenol blue, 20% glycerol) buffer was added, and samples were boiled for 5 min. Expressed products were analyzed by SDS-PAGE on a 12% gel.

Inclusion bodies were purified as follows: pET17-DHFR cultures were grown in LB containing carbenicillin (50 µg/ml, Sigma, St. Louis) and thymine (100 µg/ml, Sigma, St. Louis) to a OD<sub>600nm</sub> of 0.8, and induced as above. Cultures were grown for 4 hours post-induction, and harvested by centrifugation. Pellets were resuspended in Buffer A (15 ml) comprising of 20 mM Tris pH 7.5, 20% sucrose and 1 mM EDTA. After incubation on ice for 10 min, cells were centrifuged for 5 min at 4,000xg, and resuspended in 15 ml of ice cold water. Spheroplasts were pelleted by centrifugation at 8,000xg for 10 min and resuspended in Buffer P (3 ml) consisting of PBS, 1 µg/ml leupeptin, 20 µg/ml aprotinin and 0.5 mM PMSF (Boehringer-Mannheim, Mannheim). Samples were sonicated at 50W on a Branson Sonifier (Branson Scientific, Danbury) with 3 cycles of 15s sonication followed by 15s incubation on ice. RNase A (10 µg/ml) and DNase I (50 µg/ml, Boehringer-Mannheim, Mannheim) were added and samples were incubated at room temperature for 10 min. Samples were diluted up to 15 ml with buffer P, and centrifuged at 30,000xg for 30 min. Pellets were resuspended in buffer W (15 ml) consisting of PBS, 25% sucrose, 5 mM EDTA and 1% Triton X-100. After incubation on ice for 10 min, samples were centrifuged at 25,000xg for 10 min. Pellets were resuspended in denaturing solution D (10 ml) consisting of 20 mM potassium phosphate pH 7.0, 0.1 mM

EDTA, 0.2M KCl and 6M guanidine HCl. The suspension was stirred gently overnight at 10°C. The DHFR protein was renatured by dropwise dilution with buffer A containing 0.2M KCl and 20% glycerol (200ml). Precipitates were removed by centrifugation at 10,000xg for 30 minutes.

To assay for enzymatic activity, a NADPH-coupled test was used. When dihydrofolate is reduced to tetrahydrofolate by DHFR, NADPH is converted to NADP<sup>+</sup> with a resulting decrease in absorbance at 340nm. Dihydrofolate was prepared as follows: Folic acid (38.2mg) was dissolved in 1M NaOH (1.6ml) and added to 10% ascorbate pH 6.0 (10ml). Sodium dithionite (400mg) was added and the reaction stirred for 5 min in an ice bath. HCl (1M) was added until the pH reached 2.8, and the reaction was stirred for another 10 min. The reaction was centrifuged for 5 min at 1,000xg with a temperature of 0°C, and the precipitate redissolved in 10% ascorbate pH 6.0 (10ml). 1M HCl was added until the pH reached 2.8, and the reaction was centrifuged for 5 min at 1,000xg with a temperature of 0°C. The precipitate was dissolved in 5mM HCl (10ml), and stored in the dark at 4°C. The enzyme assay was done in reaction buffer consisting of 0.5M potassium phosphate pH 7.5, 0.3mM mercaptoethanol, 10mM NADPH (Boehringer-Mannheim, Mannheim) and 2mM dihydrofolic acid. Bovine DHFR (Sigma, St. Louis) was used as a positive control. The decrease of NADPH was monitored at 340nm in a Shimadzu spectrophotometer (Shimadzu, Columbia).

#### 2.2.1.2 The pTrxFus system

DHFR was cloned in the pTrxFus system due to its ability to enhance the solubility of recombinant systems. The synthetic DHFR gene was excised from pET17 by PCR. Two primers were designed incorporating restriction sites: DHFR1 with a KpnI site 5'-CGG **GGT ACC** AAT GAT GGA ACA GGT TTG-3' and DHFR2 with a Sall site 5'-ACG **CGT CGA** CIT AGT TGT TGG TTT TTT TTG-3'. pET17 was digested with EcoRI before use as template. The PCR reaction was conducted with 0.01 $\mu$ g of template using 1 cycle of denaturation at 95°C for 3 min, annealing at 60°C for 30s and extension at 72°C for 1 min. This was followed by 29 cycles with denaturation at 95°C for 30s, annealing at 60°C for 30s and extension at 72°C for 1 min. The PCR product was visualised by ethidium bromide staining of a 1% agarose gel. The band of approximately 800bp was excised, and purified on a Qiagen gel extraction

column according to the manufacturer's instructions (Qiagen, Hilden).

A sticky-blunt ended cloning strategy was used. The pTrxFus plasmid (2 $\mu$ g, Invitrogen, Carlsbad) was digested with Sall (20U) for 2 hours, and the enzyme heat inactivated at 70°C for 10 min. dNTP's were added to 5mM, followed by the addition of Klenow fragment (Boehringer- Mannheim, Mannheim) to the plasmid and the reaction was incubated at room temperature for 30 min. The enzyme was heat inactivated at 70°C for 10 min and the plasmid ethanol precipitated. The plasmid was subsequently digested with KpnI (20U) for 2 hours, followed by heat inactivation and gel purification. PCR product (2 $\mu$ g) was treated with T4 kinase (Boehringer-Mannheim, Mannheim) and ATP for 1 hour at 37°C, followed by heat inactivation. dNTP's were added to 5mM, followed by the addition of Klenow fragment (Boehringer- Mannheim, Mannheim) and the reaction was incubated at room temperature for 30 min at 37°C. The enzyme was heat inactivated and ethanol precipitated. The PCR product was subsequently digested with KpnI (20U) for 2 hours 37°C, and ethanol precipitated. Sticky/blunt-ended ligation was performed with 100ng of plasmid and 50 ng of PCR product using the Epicentre Fast Ligation Kit according to the manufacturer's instructions. Transformation was performed in competent G1724 *E. coli* cells (Invitrogen, Carlsbad). Colonies were screened for the presence of insert by digestion with PstI for 3 hours, and agarose gel analysis. Positive clones were sequenced with the Big Dye Kit (Perkin-Elmer, Foster City) on a ABI 377 sequencer according to the manufacturer's instructions.

Cultures bearing pTrxFus-DHFR were grown overnight in RM-medium consisting of Na<sub>2</sub>HPO<sub>4</sub> (6g/l), KH<sub>2</sub>PO<sub>4</sub> (3g/l), NaCl (0.5g/l), NH<sub>4</sub>Cl (1g/l), casamino acids (20g/l), MgCl<sub>2</sub> (0.095g/l), 50% glycerol (20ml/l) and ampicillin (50 $\mu$ g/ml). Subsequently, 0.5ml of the culture was inoculated in 20ml of induction medium consisting of Na<sub>2</sub>HPO<sub>4</sub> (6g/l), KH<sub>2</sub>PO<sub>4</sub> (3g/l), NaCl (0.5g/l), NH<sub>4</sub>Cl (1g/l), casamino acids (Gibco, 2g/l), MgCl<sub>2</sub> (0.095g/l), 20% dextrose (25ml/l) and ampicillin (50 $\mu$ g/ml) and grown to a OD<sub>600nm</sub> of 0.5. Expression was induced by the addition of tryptophan (to 100 $\mu$ g/ml) and the culture was grown for a further 4 hours. Samples were centrifuged to obtain bacterial pellets, and were resuspended in 500 $\mu$ l osmotic shock solution #2 consisting of 20mM Tris pH 8.0 and 2.5mM EDTA. Samples were sonicated with three 15 s bursts as above, and flash frozen in a methanol bath. After thawing two more sonication-freeze-thaw cycles were performed. Soluble and

insoluble fractions were separated by centrifugation at 12,000xg for 10 min at 4°C. Expression was analyzed by SDS-PAGE on a 12% gel.

### 2.2.1.3 The pET32 system

DHFR was cloned into the pET32 system, as this system is designed to produce soluble products under control of the T7 promoter. The synthetic DHFR gene was excised from pET17-DHFR by PCR. Two primers were designed incorporating restriction sites: DHFR3 with a NcoI site 5'-GCA TGC **CAT GGG** TAT GAT GGA ACA GGT TTG-3' and DHFR4 with a BamHI site 5'-CGC **GGA TCC** TAT TAG TTG TTG GTT TTT TTG-3'. pET17-DHFR was digested with EcoRI before use as template. The PCR reaction was done with 0.01 µg of template using 1 cycle of denaturation at 95°C for 3 min, annealing at 60°C for 30s and extension at 72°C for 1 min. This was followed by 29 cycles with denaturation at 95°C for 30s, annealing at 60°C for 30s and extension at 72°C for 1 min. The PCR product was visualised by ethidium bromide staining of a 1% agarose gel. The band of approximately 800bp was excised, and purified by silica-based gel extraction with melting in 6M sodium iodide, washing in Wash Solution consisting of 10mM Tris pH 7.5, 2.5mM EDTA, 50mM NaCl, 50% ethanol and elution in water (Smith *et al.*, 1995). The pET32 plasmid (2 µg, Novagen) as well as the PCR product were digested with NcoI (20U) for 20 hours, and heat inactivated at 70°C for 10 min. After ethanol precipitation, digestion was performed with BamHI (20U) for 2 hours at 37°C, followed by heat inactivation at 70°C for 15 min, followed by gel purification. Ligation was performed with 100ng of plasmid and 50 ng of PCR product using the Epicentre Fast Ligation Kit according to the manufacturer's instructions. Transformation was performed in competent BL21(DE3) or AD494 *E. coli* cells (Novagen, Madison). Colonies were screened for the presence of insert by digestion of the plasmids with PstI for 3 hours, and agarose gel analysis. Positive clones were sequenced with the Big Dye Kit on a ABI 377 sequencer according to the manufacturer's instructions.

Cultures bearing pET32-DHFR were grown to a  $OD_{600nm}$  of 0.8 and expression was induced by the addition of IPTG to a final concentration of 0.4mM. Cultures were grown for 4 hours post-induction, and bacteria harvested by centrifugation. The pellet from 10ml of culture was suspended in TE buffer (500 µl). DNaseI was added to 50 µg/ml together with 1/10th volume of 1% Triton X-100. Samples were sonicated as

described above. Soluble and insoluble fractions were separated by centrifugation at 12,000xg for 15 min. Pellets were resuspended in 1ml of 1xSDS buffer, and an equal volume of 2x SDS buffer was added to supernatants. Samples were boiled for 5 min and expression was analyzed by SDS-PAGE on a 12% gel. This procedure was performed at 37°C, 30°C and 25°C.

## 2.2.2 Expression of triosephosphate isomerase

### 2.2.2.1 The pET15b system

RNA was isolated from parasite isolate PfUP1 with the Tri-Reagent method (Molecular Research Center, Cincinnati) according to the manufacturer's instructions. Total RNA was used for reverse transcription, and TIM cDNA was amplified by PCR employing TIM-specific primers TIM1 5'-**CAT ATG** GCT AGA AAA TAT TTT GTC G-3' and TIM2 5'-**GGA TCC** TTA CAT AGC ACT TIT TAT TAT ATC-3'. Total RNA (5µg) was incubated with TIM2 (2pmol) at 70°C for 10 min, and chilled on ice. To the 10µl mix was added 5x RT buffer (4µl), 0.1M DTT (2µl) and 2.5mM dNTPs (4µl), followed by incubation at 42°C for 2 min. Superscript II(200U, Gibco, Rockville) was added, and the reaction incubated at 42°C for 50min, followed by heat inactivation at 70°C for 15 min.

A PCR reaction was set up containing cDNA (0.5 µl/1.5 µl), 10x ExTaq buffer (5µl), 5mM dNTPs (4µl), primer TIM1 & 2 (10pmol each), H<sub>2</sub>O (38µl) and ExTaq DNA polymerase (Takara, 0.3µl, Takara, Osaka). Amplification (25 or 35 cycles) was performed with denaturation at 94°C for 45s, annealing at 50°C for 1 min and extension at 72°C for 1 min. Samples were analyzed by agarose gel electrophoresis and ethidium bromide staining. The TIM PCR product was recovered from the gel by silica purification, and polished as follows: PCR product (4µl), 5mM dNTPs (1µl), reaction buffer (1.3µl), H<sub>2</sub>O (5µl) and Pfu polymerase (Stratagene, 1U) were incubated at 72°C for 30 min.

Blunt-ended ligation was performed with PCR product (250ng), pCR-Script vector (100ng, Stratagene, La Jolla), buffer (1µl), rATP (0.5µl), SrfI (1U), T4 ligase (1U) and H<sub>2</sub>O (4µl) in a total volume of 10µl at room temperature for 1 hour according to manufacturer's instructions, followed by heat inactivation at 70°C for 15 min. Transformation was performed in competent DH5α *E. coli* cells. Colonies were screened for the presence of insert by digestion with HindIII for 3 hours at 37°C,

and agarose gel analysis. Positive clones were sequenced with the Big Dye Kit on a ABI 377 sequencer according to the manufacturer's instructions.

The TIM gene was transferred to pET15b for expression. pET15b vector (Novagen, 3 $\mu$ g) as well as pCRScript-TIM (3 $\mu$ g) was digested with NdeI (30U) for 20 hours at 37°C. Following ethanol precipitation samples were digested with BamHI (30U) for 2 hours at 37°C, and purified by gel extraction with silica according to the GeneClean Kit instructions (BIO101, Carlsbad). Ligation was performed with pET15b (250ng), TIM (200ng), 10x ligation buffer (1.5 $\mu$ l), rATP (1.5 $\mu$ l) and Epicentre Rapid Ligase (1U) in a final volume of 15 $\mu$ l for 5 min at room temperature. Transformation was performed in competent BL21(DE3) *E. coli* cells. Colonies were screened for the presence of insert by digestion with HindIII for 3 hours at 37°C, and agarose gel analysis. Positive clones were sequenced with the Big Dye Kit on a ABI 377 sequencer according to the manufacturer's instructions.

Cultures bearing pET15b-TIM were grown to a OD<sub>600nm</sub> of 0.8 and expression was induced by the addition of IPTG to a final concentration of 0.4mM. The procedure was performed either at 37°C or 30°C. Cultures were grown for 0, 8 and 16 hours post-induction, and bacteria harvested by centrifugation. The pellet from 10ml of culture was suspended in TE buffer (500 $\mu$ l). DNaseI was added to 50 $\mu$ g/ml together with 1/10th volume of 1% Triton X-100. Samples were sonicated as described above. Soluble and insoluble fractions were separated by centrifugation at 12,000xg for 15 minutes. Pellets were resuspended in 1xSDS buffer (1ml), and an equal volume of 2x SDS buffer was added to supernatants. Samples were boiled for 5 min and expression was analyzed by SDS-PAGE on a 12% gel.

#### **2.2.2.2 Analysis of recombinant TIM**

Recombinant *P. falciparum* TIM was purified by immobilised metal affinity chromatography (IMAC). Culture (100ml) bearing pET15b-TIM were grown to a OD<sub>600nm</sub> of 0.8 at 30°C and expression was induced by the addition of IPTG to a final concentration of 0.4mM. Cultures were grown for 4 hours post-induction, and bacteria harvested by centrifugation. Pellets were resuspended in ice-cold binding buffer (4ml) consisting of 5mM imidazole, 0.5M NaCl and 20mM Tris pH 7.9. DNaseI was added to 50 $\mu$ g/ml, and the sample was sonicated as described

above. After centrifugation at 40,000xg for 25 min at 4°C, the supernatant was filtered through a 0.45µm filter (Waters, Massachusetts). The IMAC column (bedvolume 2.5ml, Novagen, Madison) was washed with water (3 column volumes) at a flow speed of 10 column volumes per hour and charged with 50mM NiSO<sub>4</sub> (5 column volumes) followed by equilibration with binding buffer (3 column volumes). The filtered supernatant was loaded, and the column washed with binding buffer until baseline absorbance was restored. Wash buffer consisting of 60mM imidazole, 0.5M NaCl and 20mM Tris pH 7.9 was added until a contaminant peak had appeared and baseline was restored. Recombinant TIM was eluted with elution buffer consisting of 1M imidazole, 0.5M NaCl and 20mM Tris pH 7.9 and glycerol was added to a volume of 20% for storage at 4°C. Purified TIM was analyzed by SDS-PAGE as described above.

Amino acid analysis for quantitation purposes was performed on a Pico-Tag system (Waters, Bedford) according to the manufacturer's instructions. Mass spectrometry was performed on a DE-PRO MALDI (matrix assisted laser desorption ionisation mass spectrometer, PerSeptive Biosystems, Framingham). The assay used is based on the conversion of glyceraldehyde-3-phosphate (GAP) to dihydroxyacetone phosphate (DHAP) coupled to  $\alpha$ -glycerolphosphate-dehydrogenase, resulting in the conversion of NADH to NAD<sup>+</sup>. Kinetic measurements were performed at 25°C on a Shimadzu UV-5000 spectrophotometer with a constant temperature attachment. GAP was purchased in the diethylacetal monobarium form (Sigma, St. Louis) and deprotected according to the manufacturer's instructions. The concentration of the L-isomer was determined in a GAP to 3-PGA conversion assay according to instructions. All assays were carried out in a total volume of 1ml. The reaction buffer consisted of 20mM triethanolamine pH 7.9 and 1mM EDTA. The GAP substrate was used at concentrations between 0.2 and 5mM. Glyceraldehyde-3-phosphate dehydrogenase (Boe, Mannheim) was added to a concentration of 10µg/ml. The reaction was started by addition of TIM, and absorbance decrease of NADH was followed at 340nm. The pH optimum was measured in the range of 6-10, and temperature stability was measured in the range of 25-70°C by preincubation in a PTC200 thermal cycler (MJ Research, Waltham). MES buffer was used in the pH 6-7 range, 20mM triethanolamine in the 7-8 pH range and Tris in the 8-10 pH range.

## 2.3 Results

### 2.3.1 Expression of dihydrofolate reductase

Expression of the synthetic malaria DHFR gene was first done in the pET17 expression system as described by Sirawaraporn *et al.* (1993). This system expresses recombinant proteins under control of the *lac* promoter, with strict control possible by co-transformation with the pLysS plasmid, leading to the expression of small amounts of T7 lys-ozyme which is an inhibitor of T7 RNA polymerase. After induction, expression was monitored by SDS-PAGE (Figure 2.1). The recombinant DHFR protein was expressed in the induced *E. coli* strain at concentrations of approximately 1mg/ml. The distribution between soluble and insoluble fractions was not investigated at this time, since DHFR had already been described by the original authors to accumulate in the insoluble phase.

Purification of the DHFR inclusion bodies was performed according to the method described by Sirawaraporn (1993). Crude refolded DHFR was assayed for activity above the background level of that of the host *E. coli* strain (Figure 2.2).

The negative control (water) showed no DHFR activity. The control bovine DHFR showed the expected high activity, and crude refolded DHFR showed some activity. Further kinetic analysis was not performed, as it was decided to attempt to find a system which could express DHFR in a soluble form without undergoing a refolding process.

Malaria DHFR was subsequently cloned in the pTrxFus system which is designed to express a recombinant protein as a N-terminal fusion protein with *E. coli* thioredoxin to enhance solubility (LaVallie *et al.*, 1993). PCR rescue of the synthetic DHFR gene from the pET17-DHFR vector yielded a sharp band at the correct molecular mass (not shown). After recloning, transformation of pTrxFus-DHFR in *E. coli* G1724 cells yielded 3 colonies containing the correct insert. The sequence was verified by automated nucleotide sequencing. SDS-PAGE analysis of the control containing native pTrxFus and samples containing pTrxFus-DHFR transformed bacteria could not detect any expression of recombinant DHFR at temperatures of 30°C or 37°C (results not shown).

The pET32 system was tested for the expression of recombinant malaria DHFR. Similar to pTrxFus, the pET32 system expresses recombinant proteins as a N-terminal fusion protein with thioredoxin, but

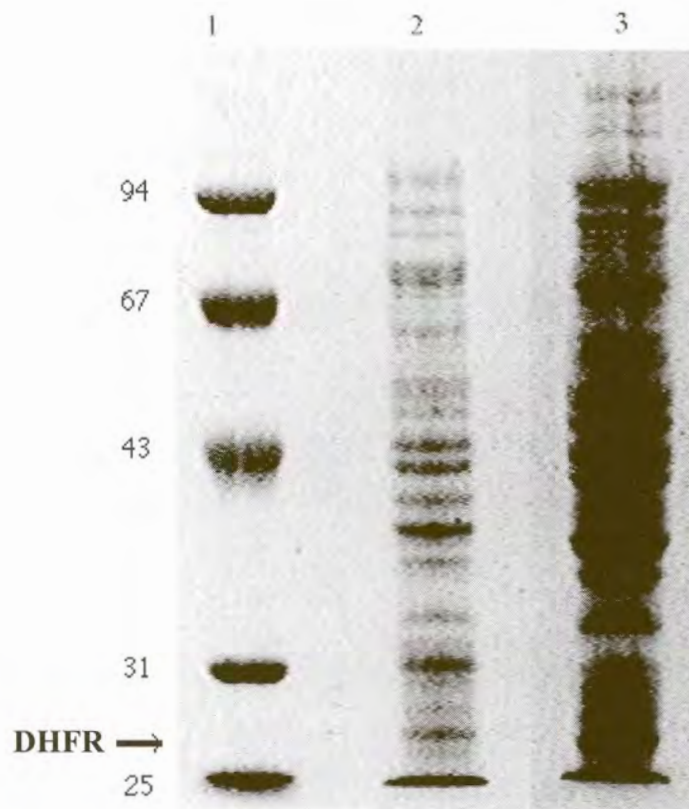


Figure 2.1: SDS-PAGE analysis of pET17-DHFR expression. Lane 1 contained molecular mass markers, lane 2 was a negative control BL21(DE3) sample and lane 3 was an extract of BL21(DE3) expressing malaria DHFR.

employs a different promoter. PCR rescue with pET17-DHFR was done as described above. Following ligation in pET32, transformation in *E. coli* BL21(DE3) cells yielded 4 colonies containing the correct insert. The sequence was verified by automated nucleotide sequencing and shown to be correct. Expression with the pET32-DHFR fusion protein at 37°C was analyzed separately for the insoluble and soluble fractions together with controls containing only pET32. A band was expected at approximately 43kDa, as the fusion proteins includes thioredoxin, two His-tags, a S-tag, a thrombin cleavage site and an enterokinase cleavage site. Very high levels of recombinant DHFR were visible at the correct molecular mass, but almost all protein was once again in the insoluble fraction (Figure 2.3).

This was repeated at a temperature of 30°C, as well as with AD494 *E.*

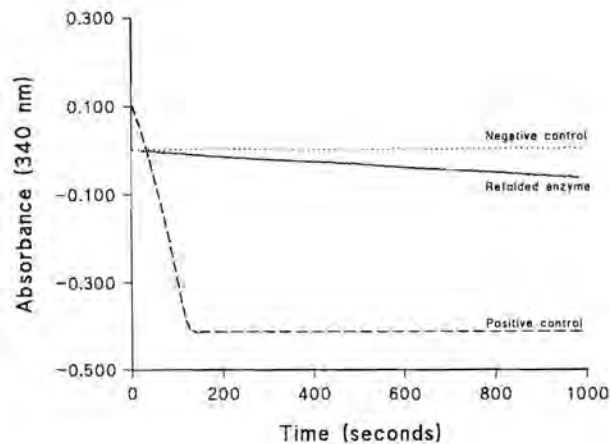


Figure 2.2: Activity assay of crude malaria DHFR. The negative control (water) is indicated by a dotted line, the positive control (bovine DHFR) by a dashed line and malaria DHFR by a solid line.

*coli* cells which are capable of forming disulfide bonds, but the results were similar to the above with little or no expression in the soluble phase.

### 2.3.2 Expression of triosephosphate isomerase

Local malaria cultures were used for RNA isolation, and selective TIM cDNA was prepared with TIM primer 2. Total RNA was used for cDNA synthesis rather than purified mRNA. When malaria total RNA is selected against poly-T oligonucleotides for enrichment of mRNA, not only the mRNA poly-A tails, but also various internal poly-A sequences from non-mRNA nucleic acids are bound. This is due to the rich AT-nature of the malaria genome. In this way the poly-T selection system is saturated, and important mRNAs may be lost. PCR with TIM cDNA as template was performed using TIM primers 1 and 2, and a sharp band of the correct size was visible at different numbers of cycles and concentrations of cDNA template (Figure 2.4). If contaminating genomic DNA had been present, it would have yielded an extra band for the intron-containing product.

The PCR product was "polished" to contain blunt ends, and was initially cloned into the pCRScript vector. The ligated construct was trans-

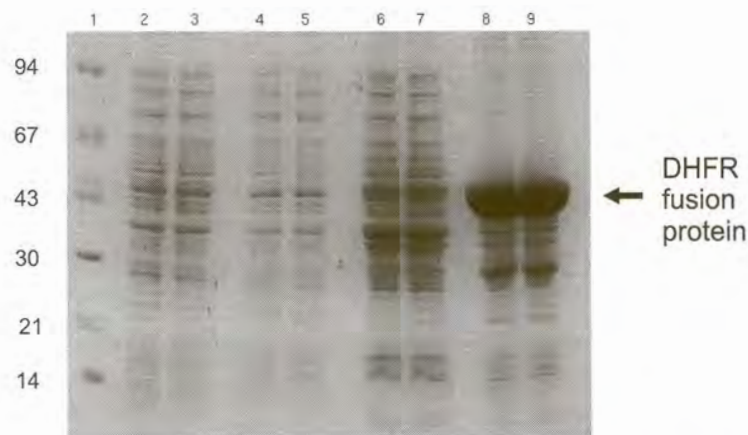


Figure 2.3: Expression of the recombinant malaria DHFR fusion protein with pET32 in BL21(DE3). Lane 1 contained molecular mass markers, lanes 2&3 both contained control soluble phases, lanes 4&5 contained soluble phases from pET32-DHFR, lanes 6&7 contained control insoluble phases and lanes 8&9 contained insoluble phases from pET32-DHFR.

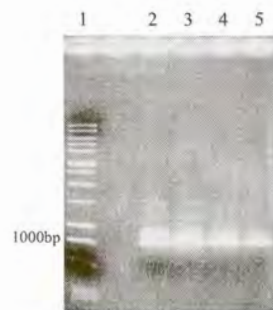


Figure 2.4: Electrophoresis of PCR products for malaria TIM. Lane 1 contained molecular mass markers, lanes 2&4 contained 1.5 $\mu$ l of cDNA template and lanes 3&5 contained 0.5 $\mu$ l of cDNA template. The PCR of samples in lanes 4&5 was performed for 35 cycles and lanes 2&3 for 25 cycles.

formed into SURE *E. coli* cells yielding 5 clones containing the correct insert. Automated sequencing showed the sequence to be identical to that reported in the literature (Ranie *et al.*, 1993) except for one silent mutation. The TIM cDNA was subsequently transferred by NdeI / BamHI restriction digestion followed by ligation to pET15b vector, yielding 2 colonies with correct inserts. Once again automated sequencing was used to verify the correct insertion and sequence of the insert. A part of the electrophoretogram for the TIM sequence is shown as an example in Figure 2.5.

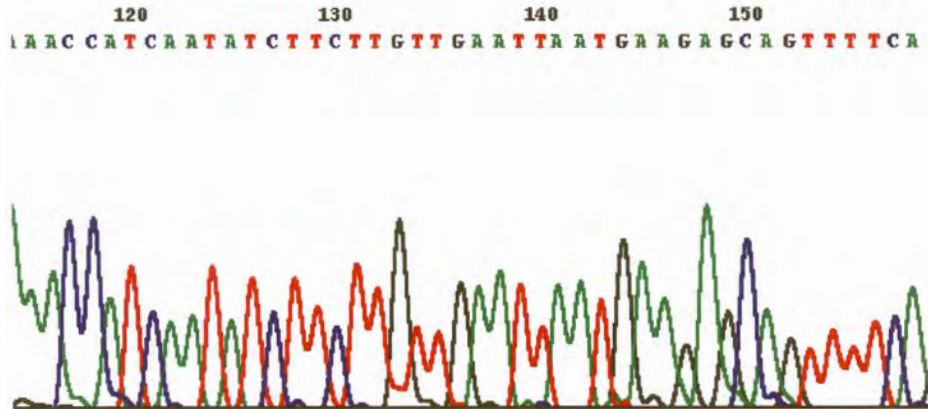


Figure 2.5: A part of the electrophoretogram for the TIM sequence.

IPTG-induced expression was monitored by SDS-PAGE at post-induction times of 0, 4, 8 and 16 hours (Figure 2.6, not all results shown). A strong band of the correct molecular mass was visible in the soluble phase with optimum expression at 8 hours post-induction. An even stronger band was also visible in the insoluble fraction indicating over-expression.

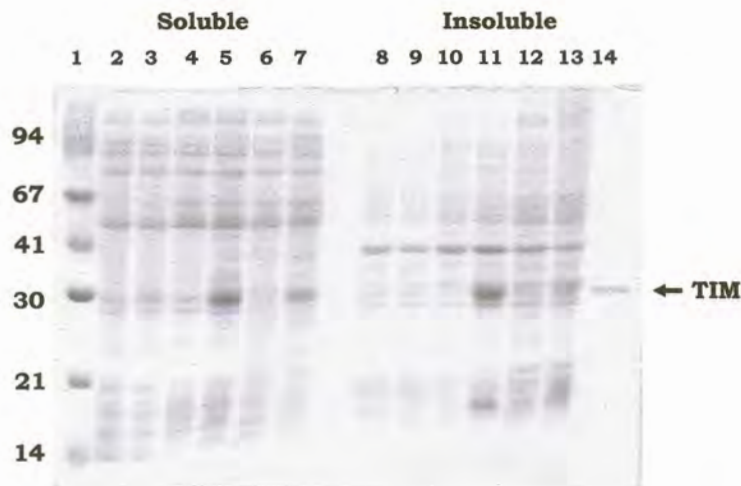


Figure 2.6: Expression of recombinant TIM at 30°C. Lane 1 contained molecular mass markers, lanes 2-7 contained soluble fractions and lanes 8-13 contained insoluble fractions. Lanes 3, 5, 7, 9, 11 and 13 contain IPTG-induced samples, and lanes 2, 4, 6, 8, 10 and 12 were uninduced. Lanes 2, 3, 8 and 9 were at 0 hours post-induction, lanes 4, 5, 10 and 11 were at 8 hours and lanes 6, 7, 12 and 13 were at 16 hours. Lane 14 contained IMAC-purified recombinant malaria TIM.

As the pET15b vector expresses the recombinant protein as a fusion

protein with a N-terminal 6 histidine tag, recombinant *P. falciparum* TIM was purified by His-tag affinity chromatography on a Ni<sup>2+</sup> chelated column. The flowthrough from the column was constantly monitored at 280nm (Figure 2.7).

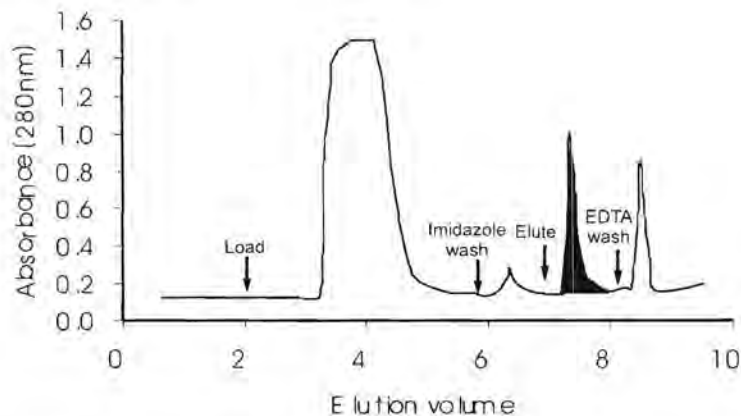


Figure 2.7: His-tag purification of recombinant TIM. The eluted recombinant protein is indicated by black shading.

Following the flowthrough of unbound *E. coli* proteins, a relatively small peak was eluted during the 60mM imidazole wash step which is optimised to elute proteins binding non-specifically to the column, possibly due to some poly-histidine residues. A large, sharp TIM peak was eluted during the 1M imidazole elution step and was collected in a volume of approximately 2ml. The column was then washed with EDTA, stripping the Ni<sup>2+</sup> and all remaining bound material from the column. Subsequent SDS-PAGE analysis of the eluted TIM showed a sharp band at the expected molecular mass, with two very faint bands (not clearly visible) at a lower molecular mass (Figure 2.6). The two faint bands may either be contaminating proteins or TIM breakdown products. The oligo-histidine motif was not removed, as modeling of the TIM dimer indicated that it would probably not interfere with dimerisation or activity (Figure 2.8).

TIM concentration was determined by amino acid analysis, yielding approximately 3mg of purified TIM per 100ml of culture. The amino acid composition for all amino acids could not be accurately determined due to the background caused by the imidazole elution step. MALDI analysis of TIM was performed to determine the exact mass of the translated product, and showed a major peak of 30,258Da which corresponds to the sum of the denatured m/z TIM monomer peak plus the 1/2m/z

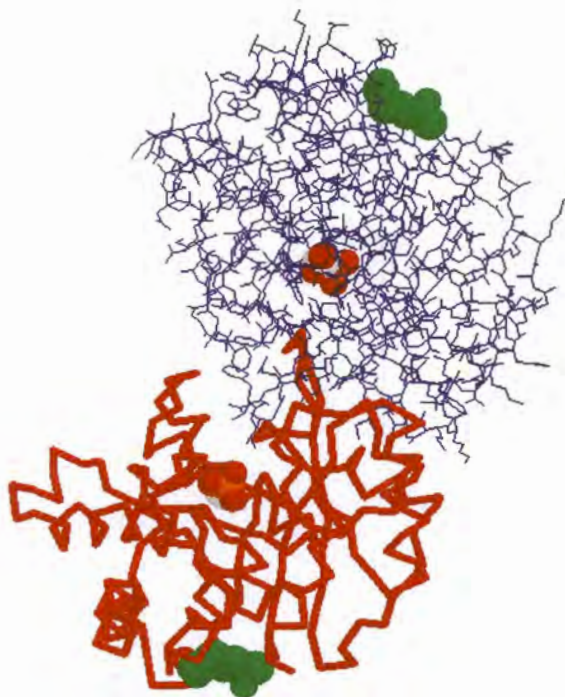


Figure 2.8: A model of malaria TIM with the subunits indicated in red and blue, the active sites in CPK-coloured spheres and the oligo-histidine tag in green.

peak of the remaining native TIM dimer. Some dimer is still visible at  $m/z=60.606\text{Da}$  (Figure 2.9).

Kinetic analysis was performed in triplicate on the recombinant TIM to determine its  $K_m$  and  $V_{max}$ , for comparison to that of TIM from other species. These values were used in an inverse reciprocal plot to calculate the kinetic parameters (Figure 2.10).

The  $K_m$  was determined as  $0.586\text{mM}$  and  $V_{max}$  as  $0.027\mu\text{mole}/\text{min}$ , which compares well to the values from other species (Table 2.2). From this data,  $K_{cat}$  was calculated as  $1.05 \times 10^5 \text{min}^{-1}$ . A specific activity of  $3913\text{U}/\text{mg}$  was calculated which is similar to those found for other isolates of *P. falciparum* TIM (Gopal *et al.*, 1999). The pH optimum for recombinant malaria TIM (Figure 2.11) was shown to be approximately 8.5 which corresponds to those determined for other species.

The temperature stability was tested by preincubation at temperatures

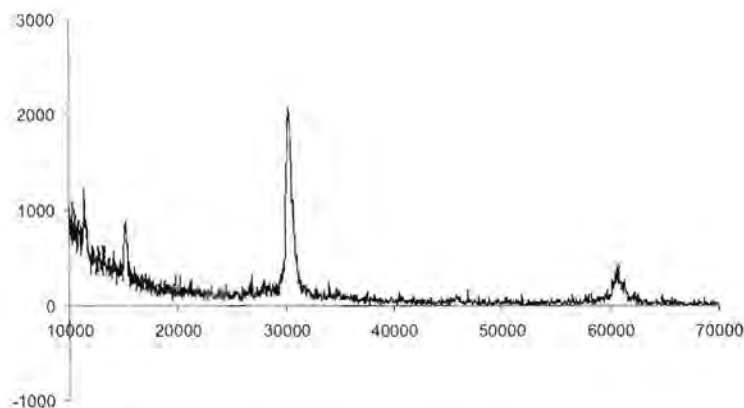


Figure 2.9: MALDI analysis of purified recombinant TIM. The major peak of 30,258Da corresponds to the sum of the  $m/z$  monomer peak plus the  $1/2m/z$  peak of the remaining dimer. Some dimer is still visible at  $m/z=60,606$ Da.

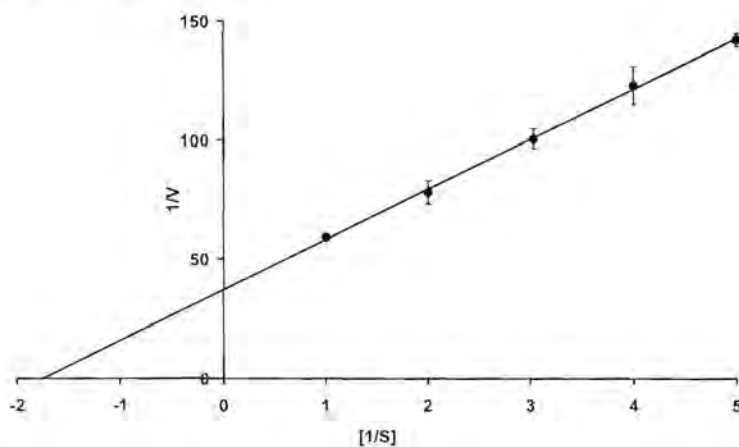


Figure 2.10: Inverse reciprocal plot for recombinant malaria TIM.  $K_m$  was determined as 0.586mM and  $V_{max}$  as  $0.027\mu\text{mole}/\text{min}$  from assays performed in triplicate.

Table 2.2: Properties of TIM from various species.

Source	$K_m$ (mM)	$K_{cot}(\text{min}^{-1})$	Reference
<i>P. falciparum</i>	0.586	$1.05 \times 10^5$	
<i>T. brucei</i>	1.2	$6.5 \times 10^4$	Lambeir <i>et al.</i> (1987)
Chicken muscle	0.97	$2.59 \times 10^4$	Putman <i>et al.</i> (1972)
	1.57	$2.92 \times 10^4$	Plaut and Knowles (1972)
Rabbit Muscle	0.39		Krietsch <i>et al.</i> (1970)
	0.32	$5.2 \times 10^4$	Hartman <i>et al.</i> (1975)
Yeast	1.22		
	1.45		Hartman and Ratrie (1977)
	1.27	$4.9 \times 10^4$	Krietsch <i>et al.</i> (1970)

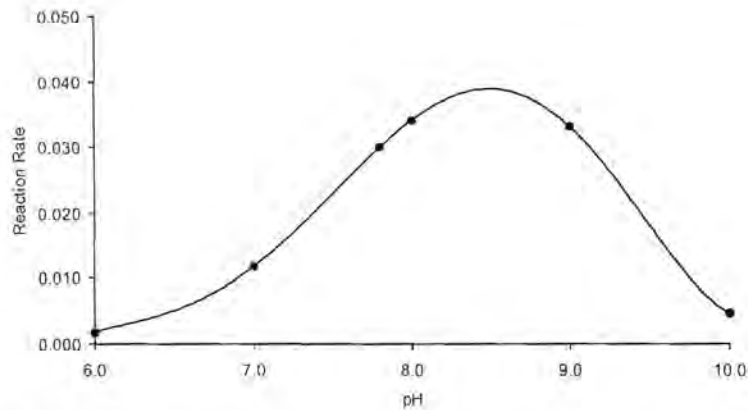


Figure 2.11: A pH optimum plot for recombinant TIM. The optimum was determined as approximately 8.5.

varying from 30 to 70°C. TIM was stable up to 55°C after which a sudden loss of activity occurred (Figure 2.12).

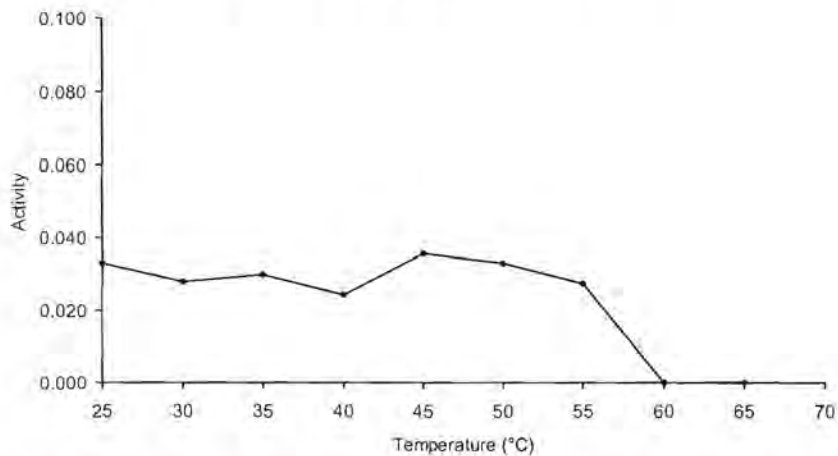


Figure 2.12: Temperature stability plot for recombinant TIM. The enzyme activity was stable to a temperature of 55°C, after which a sudden decrease in activity occurred.

## 2.4 Discussion

Expression of the synthetic DHFR gene in the pET17 vector showed an accumulation of DHFR in inclusion bodies as described in the literature (Sirawaraporn *et al.*, 1993). Overexpressed proteins often accumulate in the cytoplasm in the form of inclusion bodies that may make up a major fraction of the total cellular protein. These inclusion bodies may be separated from the rest of the cellular components due to their high density, and dissociated by detergents to extract high concentrations of a recombinant protein. However, the extracted proteins are not always correctly folded and may need denaturation and refolding. In this case, the inclusion bodies could be refolded to give approximately 20% active recombinant DHFR. Unfortunately, these type of refolding procedures are relatively variable and do not lend themselves well to the expression of proteins for complex manipulations. If mutations were to be made, comparison between native and mutated recombinant proteins would be difficult, as measured differences could not be conclusively ascribed to either the mutation or to the refolding procedure. The ideal would be to obtain large quantities of expressed active recombinant protein in soluble form that could be easily purified by employing some sort of a tag.

The pTrxFus system was initially chosen due to its ability to express recombinant proteins as N-terminal fusion proteins with *E. coli* thioredoxin. In this way the solubility of many recombinant proteins have been enhanced to give rise to a correctly folded active soluble protein (LaVallie *et al.*, 1993)(Yasukawa *et al.*, 1995)(Lunn and Pigiet, 1982). The pTrxFus system provides an enterokinase cleavage site between thioredoxin and the recombinant protein, so that the thioredoxin fusion peptide may be removed if necessary (Baratti *et al.*, 1973). pTrxFus employs a tryptophan-inducible bacteriophage  $\lambda$  major leftward promoter. Unfortunately when expression was induced in this system, no recombinant protein was visible at temperatures of 30°C or 37°C.

As expression had taken place under a T7 promoter in the pET17 system, a new expression vector was chosen. This was pET32 which contained a strong IPTG inducible T7lac promoter, and expressed recombinant proteins as N-terminal fusion proteins with thioredoxin and S-tag (a ribonuclease-S binding peptide) (Kim and Raines, 1993). The T7lac promoter carries a lac sequence just downstream from the T7 promoter, as well as the natural promoter and coding sequence for the lac re-

pressor (lacI), oriented such that the T7lac and lacI promoters diverge (Studier *et al.*, 1990). The lac repressor acts both at the lacUV5 promoter in the host chromosome to repress transcription of the T7 RNA polymerase and at the T7lac promoter in the vector to block transcription of the target gene by any synthesized T7 RNA polymerase. Thus strict control may be exercised over the expression of a recombinant protein. Even with the presence of thioredoxin, recombinant DHFR was expressed in the insoluble phase, although at very high quantities. The insolubility may be a combination of incorrect folding and overexpression of the protein.

In this study no expression system was able to express active recombinant malaria DHFR in a soluble form. However, in some recent publications alternative systems have been described. Hekmat-Nejad *et al.* (1997) described the expression of the native malaria gene for DHFR in the pET23d system employing a T7 promoter. Although the protein had to be refolded to regain activity, it was shown that the native malaria gene could be expressed at high quantities in *E. coli* if a T7 promoter was used. Expression of native DHFR-TS was attempted by Sirawaraporn *et al.* (Sirawaraporn *et al.*, 1990), but low quantities of expression led them to the use of a synthetic DHFR gene. Another publication from the Sirawaraporn group described the chemical synthesis of the complete DHFR-TS gene (Prapunwattana *et al.*, 1996). In this study the complete bifunctional DHFR-TS enzyme was expressed in *E. coli* and a correctly folded fully active enzyme was produced. From these results it thus seems that malaria DHFR is not able to fold correctly in *E. coli* in the absence of the junction and TS chains. The optimal solution seems to be the expression of the complete native DHFR-TS gene in *E. coli* under control of a T7-based promoter. The possibility of expressing proteins such as DHFR in yeast complementation systems was also demonstrated by Wooden *et al.* (1997) where yeast expressing constructs with malaria DHFR alleles were screened in terms of pyrimethamine resistance.

*P. falciparum* TIM was expressed in pET15b under the control of aT7lac promoter. This system expresses the recombinant protein as a fusion with a N-terminal motif containing 6 histidines followed by a thrombin cleavage site. TIM was expressed in quantities of approximately 5mg per 100ml of culture, with a 1:4 distribution between the soluble and insoluble phase. This may be due to weak accommodation of overexpressed TIM in the *E. coli* cytoplasm. Recombinant TIM was success-

fully purified using a  $\text{Ni}^{2+}$  chelating column, and yielded approximately 3mg of purified TIM per 100ml culture. SDS-PAGE analysis showed two other barely visible bands in the sample which may be contaminating proteins binding to the column, truncated proteins or TIM breakdown products. The recombinant protein was approximately 95% pure (densitometry) and was deemed suitable for kinetic and inhibition studies. Kinetic measurements were performed with DHAP as substrate in an NADH-linked spectrophotometric assay. The  $K_m$  was determined as 0.586mM and  $V_{max}$  as 0.027 $\mu$ mole/min, which compares well to those of other species. The increased  $K_{cat}$  of  $1.05 \times 10^5$  corresponds to the necessary increase in glycolytic activity that occurs upon infection of red blood cells with malaria parasites. A specific activity of 3913U/mg was calculated. TIM had a pH optimum of approximately 8.5 and remained temperature stable up to 55°C. The recombinant TIM was suitable for further inhibitory and mutational studies.